Journal of Structural Geology 32 (2010) 1450–1465

Contents lists available at ScienceDirect

Journal of Structural Geology

journal homepage: www.elsevier.com/locate/jsg

Magmatic structures and kinematics emplacement of the Variscan granites from Central Portugal (Serra da Estrela and Castro Daire areas)

Helena Sant'Ovaia[a,*], Philippe Olivier[b], Narciso Ferreira[c], Fernando Noronha[a], Denis Leblanc[d]

[a] Universidade do Porto, Faculdade de Ciências, Departamento de Geociências Ambiente e Ordenamento do Território, Rua do Campo Alegre 687, 4169-007 Porto, Portugal
[b] Université de Toulouse, UPS (OMP), CNRS, IRD, LMTG, 14 Avenue Edouard Belin, F-31400 Toulouse, France
[c] LNEG, Unidade de Geologia e Cartografia Geológica, Rua da Amieira, 4466-956 S. Mamede Infesta, Portugal
[d] 30, Bd Jean Brunhes F-31300 Toulouse, France

ARTICLE INFO

Article history:
Received 17 December 2009
Received in revised form
23 August 2010
Accepted 6 September 2010
Available online 16 September 2010

Keywords:
Variscan granites
AMS
Strike-slip fault
Forceful emplacement
Portugal

ABSTRACT

The late-D3 Variscan granites, which represent the most important volume of granites of Central Portugal, are studied here for their magmatic and solid-state fabrics by means of the Anisotropy of Magnetic Susceptibility (AMS) technique in a 5000 km^2 area located between Guarda and Castro Daire, including the Serra da Estrela region. Two main directions, N150E and N20E, of stretching lineations are found indicating that the emplacement of these "late kinematic" granitoids was tectonically controlled. A three-stage model is proposed in which a) openings along N150-striking dextral strike-slip faults allow the first granitic magmas to be emplaced in the upper crust of Palaeozoic metasediments and syn-D3 granitoids; b) openings along N20-striking possibly sinistral strike-slip faults conjugates to the prior strike-slip faults and allow the enlargement of the granitic plutons; and c) the final emplacement of this huge volume of granitic rocks was mainly controlled by the magma pressure, which explains the rarity of structures related to this stage of granites emplacement in the country rocks. This structural study of granitic rocks yields new constraints on the tectonic evolution of this part of the Variscan orogenic belt at c. 300 Ma.

1. Introduction

In the absence of direct geochronological evidence, correlating the deformations and the mode of emplacement of granite bodies with regional tectonic events is a challenge because granitic rocks do not always display deformation fabrics at a mesoscopic scale. Anisotropy of magnetic susceptibility (AMS) studies may be used to characterize and measure weak anisotropic fabrics (foliations and lineations), either magmatic or solid-state ones, which are essential to describe the different deformations for a granite, to identify the constraints leading to the granite intrusion, and finally to link these features to the regional tectonics.

A large area (c. 5000 km^2) of Variscan granitic outcrops, in Central Portugal between Serra da Estrela and Castro Daire massifs, was studied for this work. Despite a good geological mapping and documented geochemistry and petrography for these granites, the relationship between the emplacement of these granites and regional tectonics has so far remained unexplored. Microstructural and AMS data were gathered, described and analyzed to infer emplacement and tectonic relationships for these granites.

2. General framework

2.1. The Iberian Massif

The Iberian Variscan belt, also known as the Iberian Massif, is a large arcuate segment of the European Variscan Fold Belt which extends over more than 3000 km from eastern Germany to the Iberian Peninsula. Julivert et al. (1974) subdivided the Iberian Massif into five main zones with different geological characteristics: the Cantabrian Zone, the West Asturian Leonese Zone, the Central Iberian Zone (CIZ), the Ossa Morena Zone and the South Portuguese Zone. Later, Farias et al. (1987) included the allochthonous and parautochthonous units of the CIZ in a separate zone called the Galicia Trás-os-Montes Zone. According to this classification, the studied area is located within the autochthonous terrains of the CIZ (Fig. 1).

The Variscan orogeny was a major event in the tectonic evolution of Western Europe resulting from the Laurussia–Gondwana collision through the late Devonian and most of the Carboniferous (Ribeiro et al., 1990; Martínez Catalán et al., 2009). Its magmatic

* Corresponding author. Tel.: +351 22 0402464; fax: +351 22 0402490.
E-mail address: hsantov@fc.up.pt (H. Sant'Ovaia).

0191-8141/$ – see front matter © 2010 Elsevier Ltd. All rights reserved.
doi:10.1016/j.jsg.2010.09.003

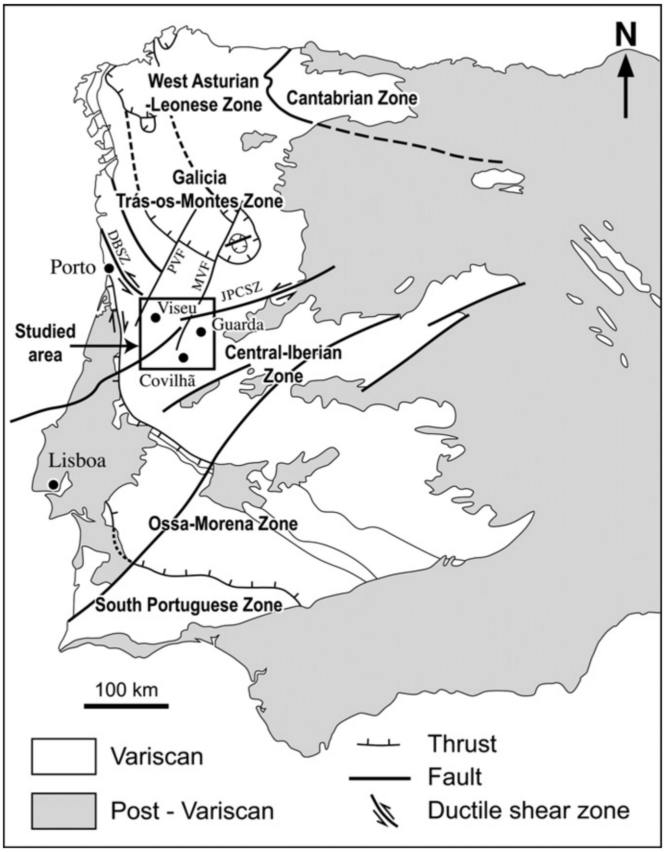

Fig. 1. Location of the studied area in the Central Iberian Zone (CIZ), part of the Variscan Chain in Western Iberia. MVF: Manteigas-Vilariça Fault; PVF: Penacova-Verin Fault; DBSZ: Douro-Beira Shear Zone; JPCSZ: Juzbado-Penalva do Castelo Shear Zone.

and tectonometamorphic features have been explained by an obduction-collision orogenic model with left lateral-transpression (Dias and Ribeiro, 1994). In the northwestern part of the Iberian Peninsula, three main phases of ductile deformation (D1, D2 and D3) have been described (Ribeiro, 1974; Noronha et al., 1979; Ribeiro et al., 1983). They are characterized by the generation of subvertical D_1 folds with a steep slaty cleavage and, particularly in the allochthonous terrains of the Galicia Trás-os-Montes Zone, D_2 recumbent folds with axial plane crenulation cleavage or schistosity associated to large thrust units or sub-horizontal extensional shear zones. Late stage D3 ductile deformation produced vertical folds with sub-horizontal axes and subvertical strike-slip shear zones, both right and left lateral. In central Portugal, especially in the studied area, the CIZ is characterized by a domain of D3 vertical folds deforming D1 sub-horizontal structures. However, earlier D1 fabrics overprinted by an extensional event prior to D3, are described in the Spanish part of the CIZ (Diez Balda et al., 1990, 1995; Escuder Viruete, 1998). A post-D3 brittle phase is characterized by a set of conjugate strike-slip faults (NNW-SSE dextral and NNE-SSW sinistral) late structures, whose geometry is often strongly influenced by pre-existent discontinuities (Ribeiro, 1974; Arthaud and Matte, 1975; Pereira et al., 1993).

Based on geological, petrographic and geochemical studies, the Portuguese Variscan granites were divided into two main groups: dominant biotite granites (biotite $>>$ muscovite) and two-mica (muscovite $>$ biotite) granites. Considering their relation with the D3 deformation phase, syn-D3, late-D3 and late to post-D3 granites were defined (Ferreira et al., 1987). The CIZ zone is characterized by huge volumes of granitic rocks that represent about 60–70% of the outcropping rocks. The syn-D3 granites are represented by two-mica peraluminous granites, granodiorites and biotite granites. The late and post-D3 granites are represented by biotite and two-mica granites, and also by gabbros, diorites, quartz-monzodiorites and granodiorites (Azevedo and Valle Aguado, 2006).

Isotopic ages for some granitoids in the Portuguese sector of the CIZ are recently published. These data are as follows:

- granitoids which have been interpreted as syn-D3 by most authors because of their strong deformation fabrics are dated in the 314–307 Ma time-span (e.g. U–Pb on zircon and monazite datations of Maceira pluton, 314 $\pm$ 5 Ma; Casal Vasco pluton, 311 $\pm$ 1 Ma; Junqueira pluton, 307.8 $\pm$ 0.7 Ma, by Valle Aguado et al. (2005) and Azevedo and Valle Aguado (2006)).
- granitoids which have been interpreted either as syn-D3 (de Carvalho et al., 1992) or late to post-D3 (Ferreira et al., 1987; Azevedo and Valle Aguado, 2006) have yielded two ages groups: (i) in the 308–301 Ma time-span (e.g. U–Pb on zircon datations of the Cota-Viseu granite: 307.7 $\pm$ 7.8 Ma and 305.2 $\pm$ 4.4 Ma by Valle Aguado et al. (2005); U–Pb or Th–Pb on monazite datations of the Cabeço do Faraó/Cabeço do Meio plutons: 302.8 $\pm$ 2.4 Ma (U–Pb) and 303.8 $\pm$ 2.4 Ma (Th–Pb), and of the Seia granite: 304.1 $\pm$ 2.9 (U–Pb) and 301.4 $\pm$ 1.6 (Th–Pb) by Neiva et al. (2009); and (ii) in the 295–287 Ma time-span: Calde granite: 294.1 $\pm$ 3.5 Ma (U–Pb on monazite) and 294.8 $\pm$ 2.9 Ma (U–Pb on zircon) by Mota Leite et al. (2005); Covilhã granite: 290.1 $\pm$ 2.4 Ma and 288.6 $\pm$ 1.5 (U–Pb and Th–Pb on monazite, respectively) by Neiva et al. (2009); Cativelos granite: 287.7 $\pm$ 2.0 Ma and 288.7 $\pm$ 1.6 Ma (U–Pb and Th–Pb on monazite, respectively) by Neiva et al. (2009). The Manteigas biotite granite considered as syn-D3 by de Carvalho et al. (1992) was dated at 481.1 $\pm$ 5.9 Ma (U–Th–Pb on zircon), i.e. early Ordovician, by Neiva et al. (2009).

The interpretation of some of these ages with respect to other geological data is difficult. For instance, the Seia and Covilhã granites, interpreted by Ferreira and Vieira (1999) as two facies with different grain size of the same granite type with very gradual transitions between them, have yielded very different ages.

Geochronological data from nearby granitoids of the Spanish sector of the CIZ are distributed in the same time-spans as those inferred for the Portuguese sector. Concerning late-D3 intrusions, Zeck et al. (2007) found ion-microprobe U–Pb ages of 305.6 $\pm$ 1.4 Ma (Navahermosa meta-gabbronorite), 306.5 $\pm$ 1.5 Ma (Colmenar cordierite bearing biotite granite) and 306.8 $\pm$ 1.9 Ma (Ledrada biotite granite). In the southern part of the CIZ, U–Pb dating of the granodiorite and granite units of the "Los Pedroches" batholith yield an age of 308 $\pm$ 2 Ma for the Los Pedroches granodiorite and 314.2 $\pm$ 1.9 Ma and 304 $\pm$ 2 Ma for Campanario La-Haba and Cerro Mogábar granites respectively (Carracedo et al., 2009). These authors proposed an emplacement for this batholith during and after D3.

2.2. Geological setting

The studied area is located between latitudes 40°15′–40°55′ N and longitudes 7°15′–8°10′ W (Figs. 1 and 2a). Most of this area is occupied by Variscan granitoids attributed to the syn- and late-D3 groups (Ferreira et al., 1987; de Carvalho et al., 1992) which are intruded into metasedimentary rocks corresponding to the autochthonous formations of the CIZ. Lithostratigraphically the metasediments are characterized by:

(a) pre-Ordovician strata which constitute a monotonous mega-sequence of metapelites and metagreywackes of uncertain age, generally referred to as the 'Complexo Xisto-Grauváquico' (CXG) (Teixeira, 1954; Sousa, 1971).

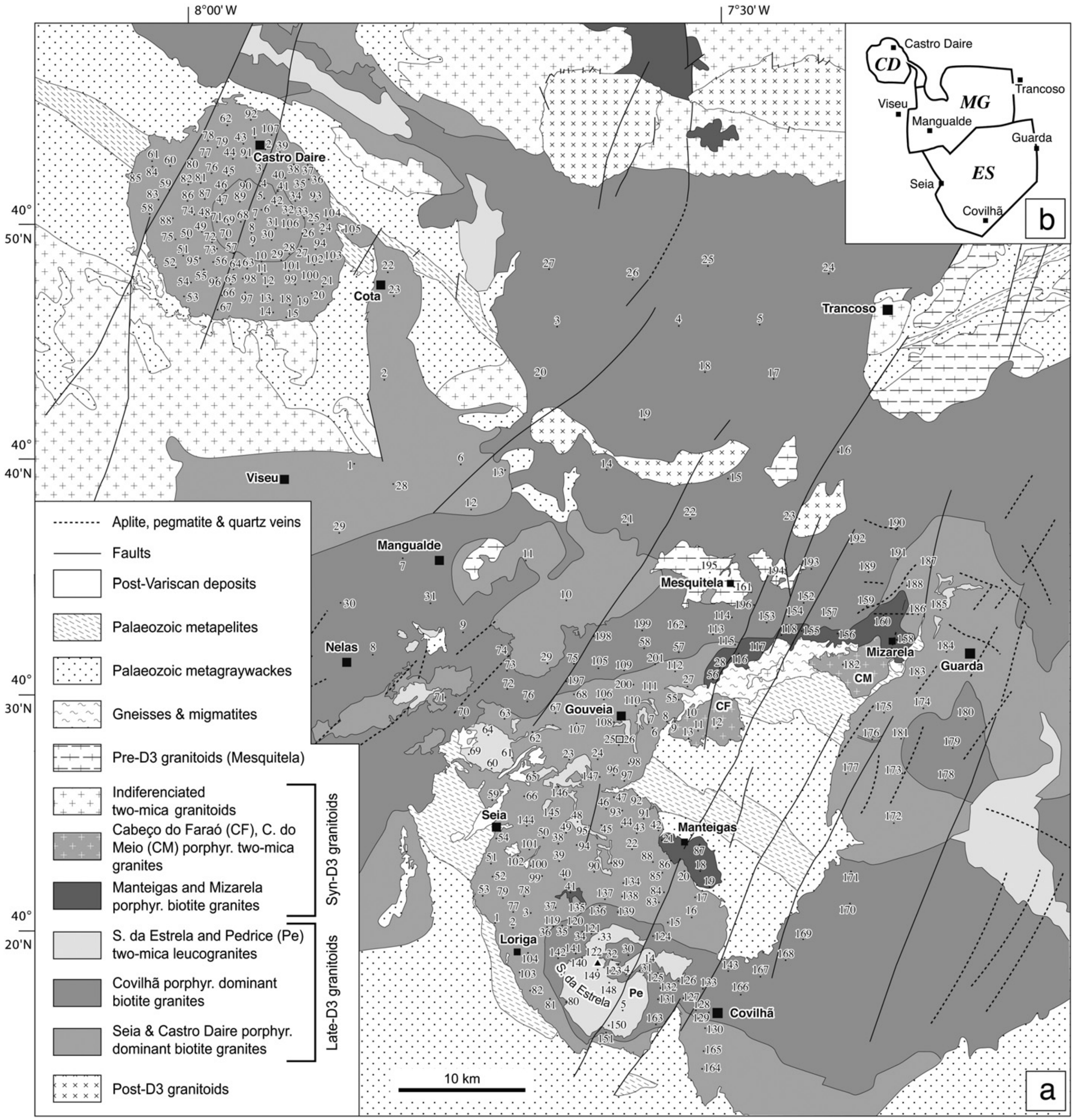

Fig. 2. a – Simplified geological map of the Serra da Estrela – Castro Daire area and sampling sites. (Modified from Schermerhorn, 1980; Ferreira et al., 1987; de Carvalho et al., 1992; Ferreira and Vieira, 1999; Azevedo and Valle Aguado, 2006). b – Sketch map of the three studied sub-zones (CD: Castro Daire; MG: Mangualde; ES: Estrela) with place names for reference to the geological map.

(b) a succession of Ordovician, Silurian, Lower Devonian and Upper Carboniferous rocks exposed in the core of the Porto-Satão Syncline (Valle Aguado et al., 2005).

The studied area contains large ductile shear zones related, at least partly, to the D3 phase (Fig. 1): (i) the NW-SE-trending Douro-Beira sinistral shear zone (DBSZ) that deforms the Porto-Satão Syncline (Ribeiro et al., 1990; Valle Aguado et al., 2005), (ii) the ENE-WSW-trending Juzbado-Penalva do Castelo sinistral shear zone (JPCSZ) (Iglesias and Ribeiro, 1981; Ferreira Pinto et al., 1993) and (iii) the NNW-SSE- to NS-trending Porto-Tomar dextral shear zone. NNE-SSW-trending brittle structures, such as the Manteigas-Vilariça fault (MVF) or Penacova-Verin Fault (PVF), are treated as later structures.

The study area (Figs. 1 and 2a) is located in the quadrilateral formed by the cities of Castro Daire – Seia – Covilhã – Guarda. For an easier description, we have subdivided this large area in three zones: Serra da Estrela (ES) to the south, Castro Daire (CD) to the north and Mangualde (MG) in between (Fig. 2b).

Table 1
AMS data for the 339 sampling sites of the Serra da Estrela – Castro Daire area.

Site nb.	*K*m (10^{-5} SI)	Ppara %	Lineation				Foliation			E12	E23	E31
			K1D	K1I	*K* 3D	*K* 3I	Az		Dip			
ES001	7.5	2.1	187	36	63	38	153	W	52	51	49	31
ES002	10.7	3.6	162	46	256	4	166	E	86	50	14	12
ES003	8.8	2.0	156	4	56	68	146	W	22	40	22	15
ES004	6.3	1.0	251	42	41	44	131	S	46	36	36	25
ES005	4.6	1.1	179	39	89	0	179	W	90	43	28	19
ES006	5.3	4.2	155	60	19	23	109	S	67	24	24	14
ES007	3.3	2.7	156	58	58	5	148	W	85	24	17	10
ES008	10.4	2.3	268	28	175	5	85	N	85	28	28	20
ES009	4.2	1.9	232	49	131	10	41	W	80	38	19	14
ES010	3.5	1.8	135	34	336	54	66	S	36	11	11	8
ES011	3.9	3.0	138	18	24	51	114	S	39	41	15	11
ES012	2.8	2.2	145	29	34	33	124	S	57	19	19	14
ES013	7.0	2.7	139	18	266	61	176	E	29	19	19	13
ES014	5.5	1.4	305	69	141	21	51	N	69	36	18	13
ES015	8.6	2.2	152	32	49	21	139	W	69	51	24	18
ES016	14.1	3.0	175	35	78	11	168	W	79	41	22	15
ES017	8.7	1.5	139	40	285	45	15	E	45	70	63	49
ES018	1673.2	15.7	162	40	37	35	127	S	55	5	5	4
ES019	27.6	2.8	140	64	40	5	130	S	85	41	14	11
ES020	11.6	3.3	284	53	59	28	149	W	62	48	22	16
ES021	27.5	4.4	304	87	99	3	9	W	87	25	25	15
ES022	10.8	2.7	317	7	51	35	141	W	55	50	29	21
ES023	7.8	2.2	338	5	81	69	171	W	21	36	36	23
ES024	10.9	2.0	103	4	2	71	92	S	19	72	29	25
ES025	12.3	2.5	208	27	3	61	93	S	29	30	30	19
ES026	5.3	3.5	212	25	56	63	146	W	27	45	12	10
ES027	4.6	3.1	147	81	345	9	75	S	81	26	26	15
ES028	20.9	1.8	30	2	298	47	28	E	43	17	17	12
ES029	6.6	4.6	141	40	339	49	69	S	41	59	11	10
ES030	10.3	2.1	152	37	302	49	32	E	41	32	23	14
ES031	2.1	0.8	27	8	288	47	18	E	43	30	30	20
ES032	4.8	1.0	169	20	284	49	14	E	41	29	29	18
ES033	2.9	1.1	17	5	279	58	9	E	32	28	23	13
ES034	7.7	2.0	280	50	188	2	98	N	88	36	17	12
ES035	6.9	1.4	244	11	337	15	67	S	75	54	45	30
ES036	7.2	1.8	2	76	119	6	29	W	84	61	41	30
ES037	9.5	1.3	154	34	278	40	8	E	50	44	44	29
ES038	10.2	3.2	187	1	87	84	177	W	6	25	25	17
ES039	8.6	2.4	129	37	301	53	31	E	37	56	16	14
ES040	8.7	2.0	179	45	316	36	46	S	54	46	41	25
ES041	6.3	6.3	159	15	16	72	106	S	18	55	11	10
ES042	8.0	3.0	166	35	71	8	161	W	82	58	24	19
ES043	10.8	3.1	146	19	54	5	144	W	85	67	25	21
ES044	13.3	2.6	247	47	33	38	123	S	52	51	19	15
ES045	10.0	3.2	205	59	33	31	123	S	59	76	26	23
ES046	10.1	2.7	268	37	17	24	107	S	66	60	20	17
ES047	9.8	3.8	152	52	35	20	125	S	70	72	21	19
ES048	4.1	4.9	238	48	125	19	35	W	71	23	19	11
ES049	11.1	3.3	114	15	5	51	95	S	39	71	15	14
ES050	16.1	2.5	137	25	294	63	24	E	27	38	24	16
ES051	12.5	3.0	171	43	292	29	22	E	61	27	27	22
ES052	9.7	3.1	169	57	306	25	36	E	65	20	20	15
ES053	7.1	3.1	157	63	253	3	163	E	87	38	35	21
ES054	12.0	3.4	161	18	265	36	175	E	54	24	24	13
ES086	14.0	3.6	269	65	81	25	171	W	65	50	21	16
ES087	1483.3	10.1	128	44	234	15	144	E	75	30	18	12
ES088	16.2	4.0	144	15	48	22	138	W	68	78	15	14
ES089	10.3	2.0	150	36	36	29	126	S	61	85	19	18
ES090	10.8	3.0	348	74	245	4	155	E	86	43	17	13
ES091	8.6	2.0	145	36	53	4	143	W	86	41	41	28
ES092	8.8	2.0	105	52	238	28	148	E	63	75	39	34
ES093	8.3	3.7	265	63	61	25	151	W	65	71	25	22
ES094	11.2	3.7	175	61	341	29	71	S	61	59	19	16
ES095	10.1	1.6	120	16	24	21	114	S	69	29	29	23
ES096	11.0	2.2	175	53	27	33	117	S	57	42	26	18
ES097	10.5	3.3	173	60	41	21	131	S	69	16	16	12
ES098	9.2	3.0	207	30	349	54	79	S	36	35	35	21
ES099	7.5	2.3	133	67	292	21	22	E	69	81	29	27
ES100	17.3	3.6	137	35	280	49	10	E	41	36	31	18
ES101	6.9	3.6	106	51	291	39	21	E	51	62	17	15
ES102	8.5	2.4	160	28	327	61	57	S	29	51	48	30
ES103	11.6	6.7	230	66	108	14	18	W	76	42	12	9
ES104	12.0	1.9	185	15	92	12	2	W	78	48	41	26
ES105	9.0	2.6	233	3	324	28	54	S	62	16	16	12
ES106	19.6	2.0	5	6	98	23	8	W	67	50	17	14
ES107	18.2	2.3	155	47	252	7	162	E	83	40	16	12
ES108	19.8	5.9	146	87	288	2	18	E	88	21	11	7
ES109	8.6	2.0	84	50	333	17	63	S	73	28	28	17
ES110	18.7	2.4	149	67	312	23	42	E	67	29	26	14
ES111	7.8	3.5	180	40	305	35	35	E	55	32	27	16
ES112	19.5	1.3	79	51	322	20	52	S	70	46	46	27
ES113	10.0	1.1	105	21	15	0	105	S	90	60	59	40
ES114	7.4	1.4	1	36	229	43	139	E	48	37	21	14
ES115	10.8	3.3	200	3	295	62	25	E	28	9	9	7
ES116	23.7	1.7	188	4	281	31	11	E	59	18	18	17
ES117	17.7	1.7	196	23	304	37	34	E	53	28	28	15
ES118	12.8	2.2	197	8	290	22	20	E	68	16	16	11
ES119	7.1	2.9	21	48	276	13	6	E	77	63	18	16
ES120	11.3	2.7	42	31	145	20	55	N	70	17	14	8
ES121	9.0	2.9	345	28	249	10	159	E	80	45	20	15
ES122	3.7	0.7	202	30	311	29	41	E	61	40	40	29
ES123	5.8	1.2	9	81	272	1	2	E	89	61	33	26
ES124	8.7	1.4	44	71	256	17	166	E	74	48	40	25
ES125	5.8	0.9	343	12	78	21	168	W	69	61	50	36
ES126	6.7	2.5	190	38	70	33	160	W	57	49	31	21
ES127	6.5	4.0	172	7	79	26	169	W	64	43	27	18
ES128	13.9	3.2	175	27	85	0	175	W	90	69	18	16
ES129	11.0	2.6	194	21	286	3	16	E	87	37	37	25
ES130	13.4	3.9	0	13	91	4	1	W	86	38	20	14
ES131	13.5	1.3	149	79	272	6	2	E	84	37	35	20
ES132	11.5	2.8	130	43	221	1	131	N	89	44	17	13
ES133	11.2	1.7	10	3	101	24	11	W	66	42	42	30
ES134	8.6	2.0	292	23	26	10	116	S	80	52	52	34
ES135	8.9	1.6	102	70	217	9	127	N	81	55	19	16
ES136	10.6	2.1	316	22	223	6	133	N	84	53	20	16
ES137	9.7	1.3	308	11	209	38	119	N	52	42	42	31
ES138	13.3	1.9	329	44	71	12	161	W	78	62	25	20
ES139	7.1	2.4	75	41	228	46	138	E	44	69	27	23

(*continued on next page*)

Table 1 (*continued*)

Site nb.	*K*m (10^{-5} SI)	Ppara %	Lineation				Foliation			E12	E23	E31	Site nb.	*K*m (10^{-5} SI)	Ppara %	Lineation				Foliation			E12	E23	E31
			K1D	K1I	*K* 3D	*K* 3I	Az		Dip							K1D	K1I	*K* 3D	*K* 3I	Az		Dip			
ES055	11.3	1.0	282	36	125	52	35	W	38	54	54	39	ES140	6.6	2.0	349	27	208	57	118	N	33	41	35	21
ES056	22.4	3.9	27	31	273	35	3	E	55	19	17	9	ES141	6.9	1.3	29	15	140	52	50	N	38	41	41	28
ES057	9.4	2.3	81	33	271	57	1	E	33	41	19	14	ES142	7.7	2.6	65	82	269	8	179	E	82	58	24	19
ES058	6.5	2.5	108	27	8	19	98	S	71	63	31	25	ES143	11.6	2.8	2	24	108	31	18	W	59	43	25	17
ES059	20.5	2.2	174	59	40	23	130	S	67	39	39	26	ES144	8.7	3.4	157	45	314	43	44	E	47	39	29	18
ES060	6.7	2.3	134	41	26	20	116	S	70	24	24	16	ES145	6.3	3.9	79	31	320	39	50	S	51	60	17	14
ES061	5.2	2.0	30	71	265	11	175	E	79	39	21	14	ES146	11.0	4.1	157	36	340	54	70	S	36	60	14	12
ES062	5.6	1.7	111	24	356	44	86	S	46	72	45	37	ES147	11.6	1.3	154	52	45	14	135	W	76	36	34	19
ES063	14.4	2.3	154	16	249	18	159	E	72	68	29	24	ES148	4.5	0.7	30	6	141	75	51	N	15	51	51	35
ES064	6.7	5.2	75	38	215	45	125	N	45	15	15	12	ES149	4.4	0.9	14	3	105	15	15	W	75	29	29	23
ES065	9.3	2.4	143	34	279	46	9	E	44	54	24	19	ES150	6.5	1.4	107	28	198	3	108	N	87	50	19	15
ES066	10.6	3.0	185	71	58	12	148	W	78	32	32	18	ES151	10.1	1.3	75	42	184	20	94	N	70	55	37	26
ES067	19.0	2.0	145	35	243	12	153	W	78	25	25	19	ES152	12.5	2.6	22	15	268	56	178	E	34	23	23	15
ES068	18.2	3.6	172	75	69	3	159	W	87	15	15	10	ES153	12.7	3.3	26	0	296	40	26	E	50	43	9	8
ES069	6.4	3.8	15	49	256	23	166	E	67	25	14	9	ES154	13.0	1.7	229	33	26	55	116	S	35	42	40	24
ES070	10.2	3.5	252	7	349	46	79	S	44	24	24	15	ES155	14.8	1.3	194	26	302	34	32	E	56	28	28	20
ES071	7.0	2.0	111	11	225	64	135	N	26	43	38	23	ES156	15.0	1.7	179	26	17	63	107	S	27	16	16	13
ES072	8.8	2.8	201	5	296	46	26	E	44	13	13	12	ES157	11.7	1.0	196	50	331	31	61	S	59	42	42	35
ES073	9.4	2.4	135	24	266	56	176	E	34	55	20	16	ES158	17.6	3.6	166	12	256	1	166	E	89	15	12	7
ES074	8.1	3.3	165	15	266	35	176	E	55	61	23	19	ES159	10.0	2.8	167	18	74	10	164	W	80	36	23	15
ES075	10.1	2.2	206	23	41	66	131	S	24	53	29	21	ES160	10.9	1.8	166	27	71	11	161	W	79	29	26	15
ES076	11.8	1.6	203	8	104	50	14	W	40	56	19	16	ES161	8.7	8.3	29	43	248	40	158	E	50	30	6	5
ES077	10.8	2.0	29	62	256	20	166	E	70	55	30	23	ES162	7.8	1.9	10	18	270	29	180	E	61	16	16	11
ES078	10.4	2.9	128	55	273	30	3	E	60	29	26	15	ES163	12.3	1.9	182	79	89	1	179	W	89	36	32	19
ES079	10.3	2.8	134	65	271	19	1	E	71	30	30	21	ES164	13.6	2.3	169	18	267	22	177	E	68	29	29	24
ES080	10.6	1.9	0	67	264	3	174	E	87	43	20	15	ES165	7.9	3.0	358	3	268	7	178	E	83	15	15	8
ES081	9.1	1.4	3	64	233	18	143	E	72	73	37	32	ES166	14.5	2.8	24	46	131	16	41	W	74	77	20	19
ES082	9.6	1.9	151	62	281	19	11	E	71	25	25	19	ES167	15.6	1.6	43	65	299	7	29	E	83	63	47	35
ES083	9.7	1.9	277	80	58	8	148	W	82	56	51	34	ES168	14.3	2.2	20	71	128	6	38	W	84	72	19	17
ES084	12.7	1.9	248	35	36	50	126	S	40	67	30	25	ES169	12.1	3.7	20	22	281	21	11	E	69	36	20	14
ES085	13.2	2.6	214	57	52	32	142	W	58	42	25	17	ES170	13.1	2.5	35	35	298	10	28	E	80	73	29	25
ES171	12.1	2.7	25	38	115	0	25	W	90	43	26	18	CD056	8.6	2.2	336	52	239	6	149	E	84	34	34	20
ES172	9.7	4.0	214	56	305	1	35	E	89	32	19	13	CD057	7.5	2.6	275	52	46	27	136	W	63	74	19	17
ES173	14.8	3.9	48	59	274	23	4	E	67	58	16	14	CD058	5.1	2.2	99	63	307	24	37	E	66	85	32	30
ES174	13.5	2.7	174	29	270	11	180	E	79	49	23	17	CD059	11.1	3.9	184	1	274	24	4	E	66	77	16	15
ES175	13.5	2.1	168	28	277	32	7	E	58	54	39	27	CD060	6.2	2.1	14	39	264	22	174	E	68	39	39	27
ES176	18.4	2.4	176	12	270	15	180	E	75	65	19	17	CD061	6.6	5.6	147	8	237	2	147	E	88	31	9	7
ES177	10.0	1.5	1	6	92	16	2	W	74	74	30	26	CD062	6.9	1.9	308	54	72	22	162	W	68	37	13	10
ES178	11.9	2.2	354	44	134	38	44	W	52	22	22	18	CD063	11.7	4.1	21	72	205	18	115	N	72	43	17	13
ES179	10.7	2.1	14	6	279	38	9	E	52	59	26	21	CD064	9.4	1.9	320	19	217	33	127	N	57	73	23	20
ES180	13.9	2.4	352	2	82	9	172	W	81	39	26	17	CD065	8.2	2.2	62	63	214	24	124	N	66	44	44	28
ES181	13.2	3.2	7	30	258	30	168	E	60	75	23	21	CD066	6.5	1.9	39	67	244	21	154	E	69	43	43	32
ES182	3.0	1.2	115	38	344	40	74	S	50	32	22	14	CD067	5.8	2.3	124	20	216	5	126	N	85	71	49	39
ES183	15.2	3.6	165	44	266	12	176	E	78	62	15	13	CD068	5.1	0.8	216	29	109	28	19	W	62	57	41	29
ES184	15.3	4.2	0	7	261	51	171	E	39	48	14	12	CD069	6.2	3.4	221	17	102	57	12	W	33	29	13	9
ES185	12.8	3.7	358	3	267	19	177	E	71	20	20	13	CD070	5.7	4.3	297	18	48	48	138	W	42	43	10	9
ES186	15.1	4.4	345	5	252	26	162	E	64	43	25	17	CD071	6.6	3.3	183	10	86	31	176	W	59	55	11	10
ES187	18.5	3.5	177	5	323	84	53	S	6	25	25	13	CD072	7.6	2.9	35	51	254	32	164	E	58	53	19	15
ES188	13.5	3.9	1	3	269	36	179	E	54	42	18	13	CD073	7.1	2.9	349	23	81	5	171	W	85	39	25	17
ES189	13.1	3.2	183	2	92	9	2	W	81	37	31	18	CD074	7.1	4.5	13	34	269	20	179	E	70	36	12	9
ES190	14.7	3.1	176	2	266	24	176	E	66	27	27	14	CD075	9.1	2.6	173	5	266	29	176	E	61	43	15	12
ES191	14.6	3.5	351	7	257	34	167	E	56	36	15	11	CD076	7.0	2.4	357	8	263	27	173	E	63	44	29	19
ES192	13.7	4.0	6	1	276	17	6	E	73	24	13	9	CD077	8.9	4.1	340	23	72	4	162	W	86	38	16	12
ES193	13.5	3.9	24	15	264	62	174	E	28	21	20	11	CD078	8.3	2.5	153	43	255	13	165	E	77	31	31	17
ES194	6.4	3.8	20	5	272	73	2	E	17	13	13	11	CD079	8.1	2.6	161	0	251	10	161	E	80	67	20	17
ES195	6.2	4.2	14	3	279	54	9	E	36	14	14	9	CD080	5.8	3.4	8	44	113	15	23	W	75	55	41	28

ES196	11.4	3.0	38	19	272	59	2	E	31	66	14	13
ES197	8.7	1.4	216	2	122	68	32	W	22	41	41	28
ES198	7.0	3.2	113	43	344	34	74	S	56	60	18	15
ES199	8.8	0.7	59	43	212	43	122	N	47	54	44	30
ES200	20.1	1.2	11	13	107	26	17	W	64	23	23	19
ES201	8.3	2.5	71	36	179	23	89	N	67	19	19	13
CD001	10.3	2.1	43	78	206	11	116	N	79	24	24	14
CD002	10.0	1.4	7	41	240	35	150	E	55	71	37	31
CD003	7.4	1.7	152	11	61	3	151	W	87	61	29	23
CD004	4.9	1.3	270	41	143	35	53	N	55	55	44	30
CD005	6.4	5.0	12	59	216	29	126	N	61	30	10	8
CD006	4.3	1.9	350	6	140	83	50	N	7	47	22	16
CD007	4.3	2.1	311	42	107	46	17	W	44	38	24	16
CD008	6.9	2.0	347	8	87	51	177	W	39	32	24	14
CD009	5.6	4.6	148	33	15	47	105	S	43	48	14	11
CD010	6.2	3.2	202	76	353	13	83	S	77	30	27	15
CD011	8.0	2.1	9	68	184	22	94	N	68	53	39	27
CD012	9.8	1.6	45	48	203	40	113	N	50	57	55	37
CD013	8.4	1.0	64	74	315	5	45	S	85	52	52	40
CD014	13.7	2.3	353	60	207	26	117	N	64	67	53	40
CD015	7.0	1.0	59	38	175	30	85	N	60	43	43	32
CD018	9.8	1.2	193	2	103	18	13	W	72	50	50	40
CD019	8.7	1.8	14	59	165	27	75	N	63	49	31	22
CD020	11.1	3.4	23	5	114	8	24	W	82	47	17	14
CD021	9.6	3.0	207	16	298	4	28	E	86	30	18	11
CD022	18.9	3.4	320	20	54	11	144	W	79	26	9	7
CD023	15.6	2.9	347	16	80	10	170	W	80	16	14	8
CD024	10.5	1.5	228	25	133	12	43	W	78	41	41	25
CD025	8.1	2.7	171	16	263	7	173	E	83	45	25	18
CD026	6.7	3.4	174	18	275	31	5	E	59	39	17	12
CD027	6.2	3.0	223	13	133	1	43	W	89	74	14	13
CD028	7.1	4.0	213	34	313	15	43	E	75	73	10	10
CD029	5.9	2.1	69	82	168	1	78	N	89	41	17	13
CD030	6.7	2.3	240	2	331	45	61	S	45	56	31	23
CD031	6.7	1.3	334	46	154	44	64	N	46	49	39	25
CD032	7.2	1.8	336	25	213	49	123	N	41	23	20	11
CD033	6.0	2.9	345	35	237	24	147	E	66	39	13	10
CD034	8.4	3.7	327	2	237	5	147	E	85	45	17	13
CD035	7.4	4.2	156	9	247	7	157	E	83	15	15	9
CD036	10.5	3.5	325	3	234	20	144	E	70	22	22	14
CD037	12.5	2.8	138	13	230	10	140	E	80	24	24	14
CD038	12.3	2.4	146	3	56	3	146	W	87	29	19	12
CD039	11.0	1.9	324	22	213	41	123	N	49	24	24	14
CD040	8.6	3.8	314	1	224	7	134	N	83	46	13	10
CD041	7.0	4.0	359	54	238	21	148	E	69	44	12	10
CD042	7.1	0.8	303	0	33	20	123	S	70	33	33	28
CD043	8.6	2.6	162	14	256	18	166	E	72	31	31	19
CD044	8.4	2.6	153	19	63	2	153	W	88	24	24	20
CD045	4.6	1.2	248	52	66	38	156	W	52	57	49	33
CD046	7.5	1.8	86	59	301	26	31	E	64	56	39	27
CD047	9.0	4.2	23	37	123	14	33	W	76	18	15	8
CD048	4.1	2.2	133	68	271	16	1	E	74	55	28	21
CD049	8.8	2.6	127	20	263	63	173	E	27	42	26	18
CD050	12.2	3.3	14	38	266	22	176	E	68	64	16	14
CD051	9.2	2.1	145	33	264	37	174	E	53	49	28	20
CD052	6.3	1.9	1	34	268	5	178	E	85	37	37	27
CD053	6.9	3.8	117	71	217	4	127	N	86	46	29	20
CD054	6.5	3.2	111	52	237	25	147	E	65	66	37	29
CD055	10.9	2.0	332	4	239	29	149	E	61	61	32	25
CD081	8.7	3.6	193	16	287	15	17	E	75	76	16	15
CD082	12.3	3.4	28	29	284	24	14	E	66	57	16	13
CD083	8.9	1.3	11	23	274	15	4	E	75	50	50	37
CD084	5.8	2.8	127	5	36	16	126	S	74	44	35	22
CD085	6.6	1.3	156	13	246	2	156	E	88	51	51	32
CD086	9.1	4.1	22	26	281	22	11	E	69	61	14	12
CD087	3.8	2.6	149	63	298	24	28	E	66	71	13	12
CD088	6.5	2.3	143	50	282	32	12	E	58	84	24	23
CD089	6.1	2.4	45	20	143	20	53	N	70	55	16	13
CD090	8.0	2.1	10	30	273	12	3	E	78	18	18	17
CD091	12.0	3.1	179	23	83	15	173	W	75	28	28	17
CD092	10.5	1.6	274	8	7	19	97	S	71	37	16	12
CD093	8.9	1.6	157	9	249	13	159	E	77	80	48	43
CD094	8.2	2.1	14	44	125	21	35	W	69	74	31	27
CD095	10.1	4.4	19	69	234	17	144	E	73	37	17	12
CD096	10.7	2.4	347	24	245	25	155	E	65	74	23	21
CD097	10.8	2.8	70	64	213	21	123	N	69	47	23	17
CD098	7.4	1.5	30	60	254	22	164	E	68	55	55	41
CD099	10.3	2.2	4	54	142	29	52	N	61	40	37	22
CD100	9.2	2.6	228	22	136	6	46	N	84	42	35	22
CD101	11.2	2.2	34	55	138	9	48	N	81	37	37	20
CD102	7.6	2.2	193	46	284	0	14	E	90	58	21	17
CD103	9.1	0.8	8	19	101	7	11	W	83	63	53	39
CD104	9.5	3.7	168	18	73	16	163	W	74	27	20	12
CD105	14.4	1.9	285	15	194	4	104	N	86	18	18	13
CD106	4.7	4.4	139	3	236	67	146	E	23	27	7	6
CD107	9.4	1.5	314	3	47	46	137	W	44	17	17	14
MG001	6.3	3.4	224	61	51	29	141	W	61	21	21	14
MG002	20.3	3.3	159	62	262	7	172	E	83	29	15	10
MG003	7.3	3.2	173	19	56	53	146	W	37	63	26	22
MG004	7.4	1.6	270	32	69	56	159	W	34	74	24	22
MG005	7.1	1.6	299	32	103	57	13	W	33	39	21	15
MG006	23.1	1.3	179	12	89	0	179	W	90	70	17	16
MG007	6.0	3.0	82	0	352	53	82	S	37	53	20	16
MG008	8.9	3.9	356	30	220	51	130	N	39	15	15	8
MG009	10.2	3.5	333	49	91	22	1	W	68	23	23	18
MG010	5.8	1.5	177	54	313	28	43	E	62	55	23	18
MG011	8.5	1.8	155	12	246	3	156	E	87	65	17	15
MG012	20.1	0.9	183	31	283	16	13	E	74	51	20	16
MG013	17.2	3.6	149	43	249	11	159	E	79	70	23	20
MG014	12.0	2.3	227	30	329	19	59	S	71	31	31	17
MG015	10.8	2.2	163	21	255	6	165	E	84	39	24	16
MG016	6.7	1.7	234	47	34	42	124	S	48	36	20	13
MG017	7.2	0.9	29	11	127	36	37	W	54	62	26	21
MG018	8.5	2.0	301	20	43	30	133	S	60	67	30	25
MG019	13.2	3.2	208	59	7	29	97	S	61	77	18	17
MG020	5.5	1.3	238	3	146	35	56	N	55	53	24	18
MG021A	2.8	3.4	240	17	115	63	25	W	27	27	8	6
MG021B	18.8	2.1	168	20	274	37	4	E	53	24	14	9
MG022	18.2	4.1	26	35	295	2	25	E	88	21	17	10
MG023	3.6	1.0	167	3	71	62	161	W	28	35	25	15
MG024	6.1	2.5	160	1	290	89	20	E	1	42	17	13
MG025	5.4	1.7	285	6	49	79	139	W	11	55	27	21
MG026	9.2	3.2	212	31	122	1	32	W	89	20	20	13
MG027	12.0	1.6	146	59	281	23	11	E	67	37	23	15
MG028	14.0	3.5	118	47	276	41	6	E	49	42	14	11
MG029	14.9	2.7	58	4	153	55	63	N	35	18	18	12
MG030	10.3	1.5	299	76	30	0	120	S	90	38	28	18
MG031	9.1	3.4	183	24	313	56	43	E	34	66	17	15

In the Serra da Estrela, the biotite-dominant granitoids are represented by Seia, Covilhã, Mizarela and Manteigas intrusions and the two-mica granitoids are represented by Estrela, Pedrice, Cabeço do Faraó, Cabeço do Meio and Mesquitela intrusions (Ferreira and Vieira, 1999). No consensus exists for the relationships of these granitoids to tectonic events. Therefore, these granitoids are grouped in combinations of their petrographic and structural features according to Schermerhorn (1980), Ferreira et al. (1987), de Carvalho et al. (1992), Ferreira and Vieira (1999) and Azevedo and Valle Aguado (2006). This grouping will be further discussed on the basis of our new results.

The Castro Daire zone corresponds to the Castro Daire biotite-dominant pluton composed of a peripheral porphyritic facies (Calde granite) and a central fine-grained two-mica facies (Alva granite) (Schermerhorn, 1980). Between the Serra da Estrela granites and the Castro Daire pluton, the central zone between Mangualde and Trancoso is known as "Granitos das Beiras" (Boorder, 1965), which is composed of a large volume of biotite-bearing and two-mica porphyritic granites. All described granites are crosscut by aplite and pegmatite veins with a variety of orientations and by dominantly NE-trending quartz veins.

3. Sampling and analytical technique

An AMS study was conducted to acquire a complete data set for the fabrics of the granites. This study is based on 339 sampling sites (Fig. 2a) distributed on a roughly kilometric grid in the Serra da Estrela and Castro Daire zones. In the Mangualde – Trancoso zone, the sampling grid is less dense with a spacing of about 4–5 km. At each site, four oriented cores (25 mm in diameter and 60–70 mm in length) were collected. Then, each core was sawed in two (eventually three) 22 mm long specimens. At least 8 specimens per station were available for magnetic measurements that were performed using a KLY-2 Kappabridge susceptometer ($\pm 3.8 \times 10^{-4}$ T; 920 Hz, AGICO, Czech Republic) at the 'Laboratoire des Mécanismes et des Transferts en Géologie' in Toulouse, France. A sequence of 15 susceptibility measurements along different orientations of each specimen allowed us to compute the orientation and magnitude of the three main axes $k_1 \geq k_2 \geq k_3$ of the anisotropy of magnetic susceptibility ellipsoid. For each site, the AGICO software enabled us to calculate the mean susceptibility Km, which is the mean of the eight (or more) individual arithmetic means $k_1 + k_2 + k_3/3$. Also calculated were the intensities and orientations of the three axes $K_1 \geq K_2 \geq K_3$, which are the tensorial means of the $k_1 \geq k_2 \geq k_3$ axes for the eight specimens, and the 95% confidence angles E12, E23 and E31 corresponding to these three axes. K_1, the long axis of the mean ellipsoid, is the magnetic lineation of the site and K_3, the short axis, is the normal to the magnetic foliation. P, the magnetic anisotropy ratio, corresponds to K_1/K_3. In this study we will use the parameter Ppara% $= ((K_1 - D/K_3 - D) - 1) \times 100$, where D ($=-1.46 \times 10^{-5}$ SI) is the diamagnetic component carried by the quartz and felspars (Rochette, 1987). This parameter, Ppara%, is more convenient than P for rocks displaying a small susceptibility for which it is necessary to subtract D, which is constant and isotropic, in order to avoid an artificial enhancement of the anisotropy (Bouchez et al., 1987). The values of Km and Ppara%, the direction and inclination of $K1$, the mean magnetic lineation, and of $K3$, the normal to the magnetic foliation, the azimuth and dip of this foliation, and the 95% confidence angles of $K1$, $K2$, $K3$ axes for each station are given in Table 1.

4. AMS data

4.1. Magnetic susceptibility values (Km)

Almost all the granites have magnetic susceptibilities less than 30×10^{-5} SI (Table 1 and Fig. 3), typical of a dominantly paramagnetic behaviour, i.e. they are magnetite-free (Rochette, 1987). In such paramagnetic granites, Km linearly correlates to the iron content, allowing a rough characterization of the petrographic type (Gleizes et al., 1993). Such a characterization is essential in this region for which few chemical analysis of the granitic rocks were published and generally not precisely located. In a frequency histogram of the magnetic susceptibility magnitude, five classes were defined for the study area (Km in 10^{-5} SI): $0 \leq K\text{m} \leq 7.5$; $7.6 \leq K\text{m} \leq 10.0$; $10.1 \leq K\text{m} \leq 15.0$; $15.1 \leq K\text{m} \leq 20.0$ and $K\text{m} > 20.0$. A Km map was then constructed to show the spatial distribution of the five classes (Fig. 3).

4.1.1. Serra da Estrela granites

The AMS study of these granites is based on 201 sampling stations. Km values range between 2.1 and 28×10^{-5} SI (Fig. 3). Small values, less than 7.5×10^{-5} SI, are essentially found in a circular zone between Loriga and Covilhã, corresponding to the muscovite >> biotite leucogranites forming the highest parts of the Serra da Estrela. These leucogranites are surrounded by a semicircular zone of granites with $7.6 \leq K\text{m} \leq 10 \times 10^{-5}$ SI, which are in turn surrounded by a discontinuous circular zone of granites with $10.1 \leq K\text{m} \leq 15.0 \times 10^{-5}$ SI (to the south and north of Loriga, between Seia and Manteigas and to the southwest and north of Covilhã). This susceptibility values interval, which corresponds to the frequency peak, is also well represented between Covilhã and Guarda and between Seia and Gouveia. The [7.6–10.0] and [10.1–15.0] classes of Km values correspond to the Covilhã and Seia porphyritic biotite-dominant granites. However, the distribution in map view of these two classes of Km values (Fig. 3) does not exactly correspond to the cartographic distribution of these two granites as admitted by previous authors (Fig. 2) (see Discussion). Finally, the greatest values ($K\text{m} \geq 15.1 \times 10^{-5}$ SI) are essentially found in small areas to the north of Gouveia and in the Manteigas and Mizarela biotite granites to granodiorites. Only two sites of the Manteigas granite display very large Km values (1483.3 and 1673.2×10^{-5} SI) typical of a ferromagnetic behaviour, probably due to the presence of magnetite grains.

4.1.2. Castro Daire pluton

The AMS study of this pluton is based on 105 sampling stations. The magnetic susceptibility values range between 3.8 and 13.7×10^{-5} SI (mean 8.1×10^{-5} SI) in the pluton, but values up to 18.9×10^{-5} SI were measured in the southeastern prolongation of the pluton near Cota (Fig. 3). The smallest values are mainly found in the Alva two-mica, fine-grained central facies ($4.3 \leq K\text{m} \leq 7.2 \times 10^{-5}$ SI) and also in a semicircular zone of the Calde facies, on the western border of the pluton ($5.1 \leq K\text{m} \leq 6.9 \times 10^{-5}$ SI). This peripheral facies is mainly characterized by values ranging from 7.5 to 10×10^{-5} SI around the Alva central facies, and the greatest values ($10.1 \leq K\text{m} \leq 13.7 \times 10^{-5}$ SI) occur especially in its northeastern porphyritic part near Castro Daire.

4.1.3. Mangualde – Trancoso area

Magnetic susceptibility data are based on 31 sampling stations. The Km values range between 3.6 and 23.1×10^{-5} SI (mean 11.0×10^{-5} SI) (Fig. 3) corresponding to different rock types. The histogram of susceptibility values shows two peaks in the classes $0 \leq K\text{m} \leq 7.5 \times 10^{-5}$ SI, corresponding to the Trancoso area, and $10.1 \leq K\text{m} \leq 15.0 \times 10^{-5}$ SI, mainly to the north of Mangualde, both corresponding to two-mica facies. The values between 7.6 and 10×10^{-5} SI are found in a large area to the south and east of Mangualde. The greatest values ($>20.0 \times 10^{-5}$ SI) are found in porphyritic biotite facies, to the north of Mangualde.

4.2. Magnetic anisotropy and microstructures

Ppara%, the paramagnetic anisotropy parameter, ranges from 0.7 to 8.3% (mean 2.5%) for the whole area (see below for the two higher anisotropies measured in the Manteigas granite) (Table 1 and Fig. 4). In a frequency histogram four classes, used for drawing the zones of equal anisotropy on the map, have been defined: Ppara % ≤ 2.0, 2.1 ≤ Ppara% ≤ 3.5, 3.6 ≤ Ppara% ≤ 5.0, Ppara > 5%. For the three zones of study, the highest frequency corresponds to the class 2.1 ≤ Ppara ≤ 3.5.

Ppara% is correlated to the finite deformation of a rock. This correlation depends on many factors (regime of deformation, mineralogical composition and grain size of the rock, etc.), therefore only a qualitative equivalence may generally be established. In the studied area, for Para ≤ 2%, the deformation is hardly visible to

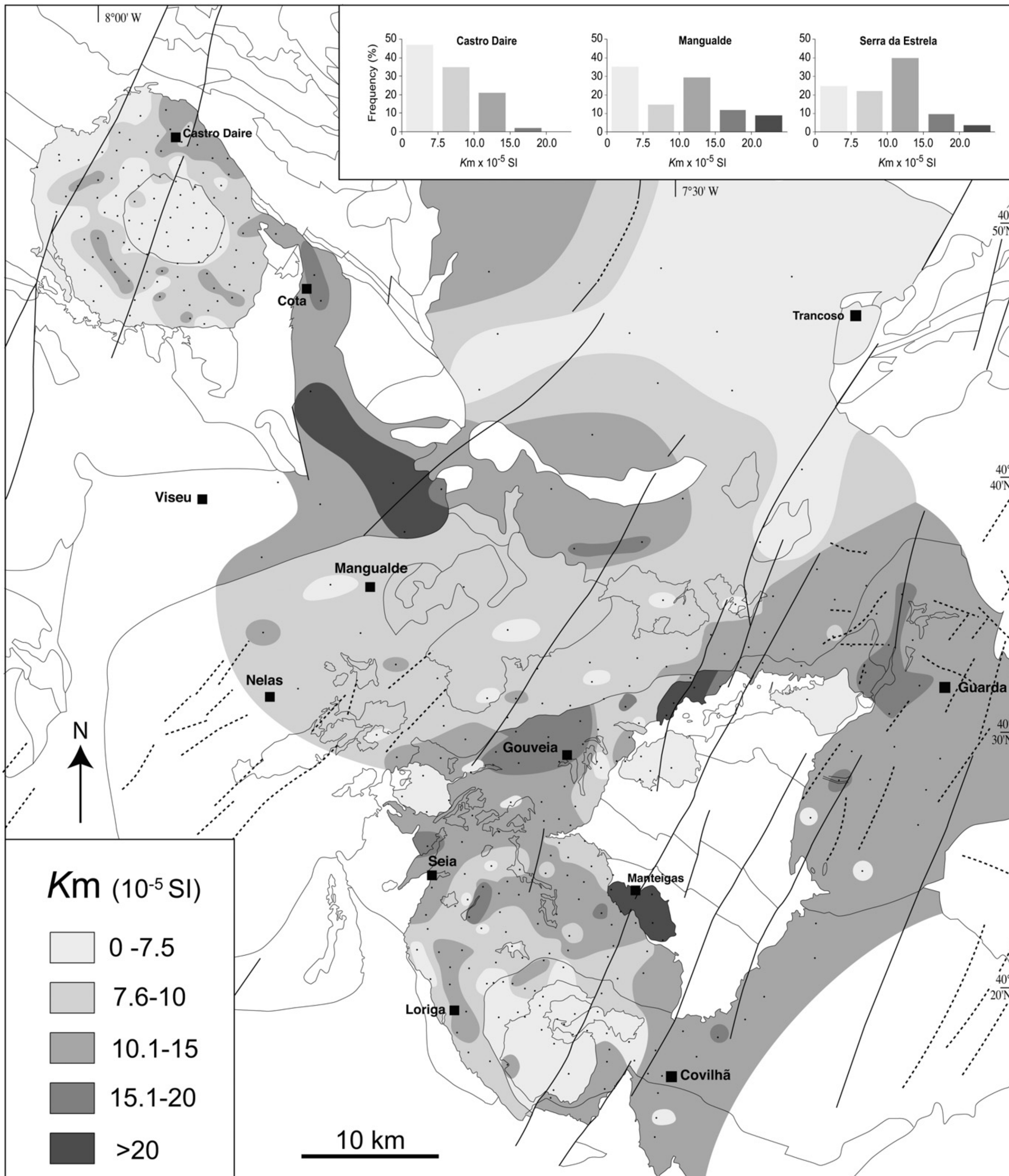

Fig. 3. Map of the magnetic susceptibility (*Km*) of the Serra da Estrela – Castro Daire area and histograms of susceptibility values for the three sub-zones.

the naked eye, for 2% < Ppara ≤ 5%, a weak orientation of the fabric may be observed, for Ppara > 5% the planar and/or linear anisotropy is well marked.

The magnetic anisotropy may correspond, in granitic rocks, either to magmatic or eventually superimposed solid-state microstructures. Criteria for this distinction have been described in the literature (e.g. Blumenfeld and Bouchez, 1988; Paterson et al., 1989, 1998; Bouchez et al., 1992) and the significance of the different microstructures is defined according to magma rheology considerations (Nicolas, 1992; Vigneresse et al., 1996).

The microstructures observed in thin sections from about half of the sampling sites in this study were grouped into four types (Fig. 5):

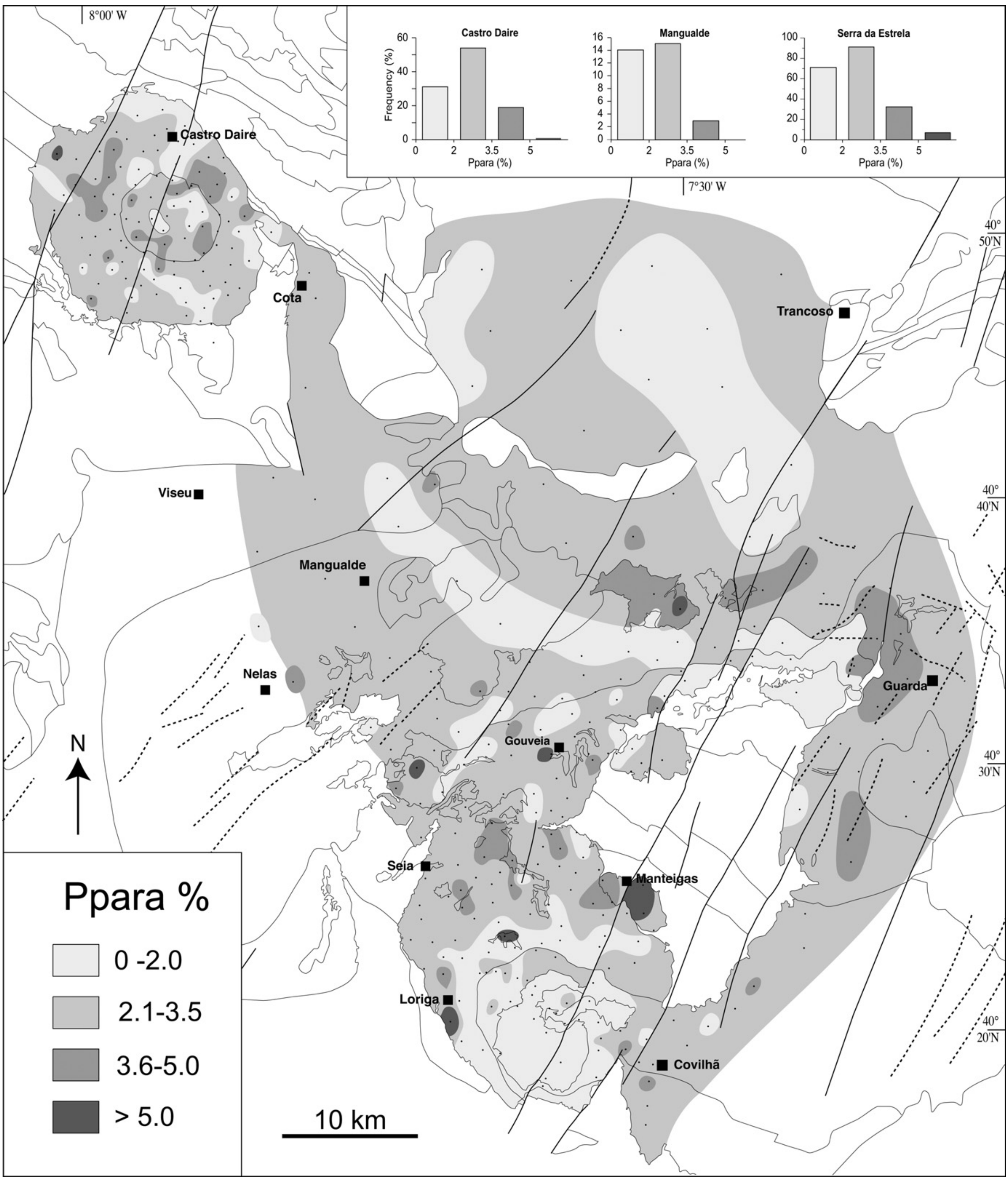

Fig. 4. Map of the anisotropy of magnetic susceptibility (Ppara%) of the Serra da Estrela – Castro Daire area and histograms of Ppara% values for the three sub-zones.

(i) magmatic microstructures (no or rare undulatory extinction in quartz); (ii) submagmatic (i.e. subsolidus) microstructures ((0001) subgrains boundaries in quartz and, eventually, folded or kinked biotites); (iii) high to medium temperature microstructures (square-shaped subgrains in quartz, recrystallized quartz grains, eventually kinked biotites and bands of quartz surrounded by mica flakes); (iv) medium to low temperature microstructures (total recrystallization of quartz grains and transformation into gneiss).

In the three studied zones, the various granite types display almost ubiquitous magmatic to submagmatic microstructures. Some high to low temperature solid-state deformation microstructures have been observed locally (see below).

4.2.1. Serra da Estrela granites

The Ppara% values range from 0.7 to 8.3% (mean 2.6%). The two highly ferromagnetic sites of the Manteigas granite have stronger anisotropies of 10.1% and 15.7%, which is probably a function of the shape anisotropy of magnetite grains. A circular zone, located in the southern part of the Serra da Estrela horst, between Loriga and Covilhã, has values between 0.7% and 2.0%. The magnetic anisotropy increases toward the periphery of this circular zone with values ranging from 2.1 to 4.9% (values >5% may be observed very locally, as 6.7% for the site ES103 to the south of Loriga), forming a zonation in the Covilhã and Seia granites (Fig. 4).

About 80% of the thin sections display microstructures corresponding to magmatic or submagmatic deformation. Microstructures corresponding to a generally slight solid-state deformation, mainly characterized by recrystallization of a part of the quartz grains, were observed especially near the contacts with the CXG country rocks of the Serra da Estrela zone, to the SE of Gouveia (sites ES6, 7, 8, 92, 96–98) and SW of Guarda (sites ES176, 177, 181). Gneissic microstructures, with quartz almost entirely recrystallized into elongated subgrains and forming continuous layers, were observed in only one site (ES128) to the west of Covilhã.

4.2.2. Castro Daire pluton

The Ppara% values range between 0.8% and 5.6% (mean 2.6%) (Fig. 4). Most sites have values between 2% and 3.5%. Small sectors to the SW and SE of Castro Daire show higher values ($3.5 \leq$ Ppara % ≤ 5), whereas the northern and southern parts of the pluton display values of Ppara% < 2. Unlike with the spatial distribution of the *K*m values, Ppara% are not arranged geometrically with respect to the pluton shape, but rather are scattered within the body.

Most sites are characterized by magmatic or submagmatic microstructures. Some sites located to the northeast of this pluton (sites CD35, 93, 104) display a moderate solid-state deformation, whereas some sites located to the northwest (sites CD61, 77, 80, 84) display textures that can be interpreted to be the result of a strong solid-state deformation, the rocks being partly transformed into gneiss (i.e. site CD61 with Ppara $= 5.6\%$, Fig. 5).

4.2.3. Mangualde – Trancoso area

Ppara% values range between 0.9% and 4.1% (mean 2.4%) (Fig. 4). Between the Castro Daire pluton and the Serra da Estrela granites most values are between 2.0% and 3.5%. Smaller values are mainly observed to the west of Trancoso and to the east and southeast of Mangualde.

Almost all sites display magmatic or submagmatic microstructures. Only four sites (MG1, 2, 14 and 15) display microstructures

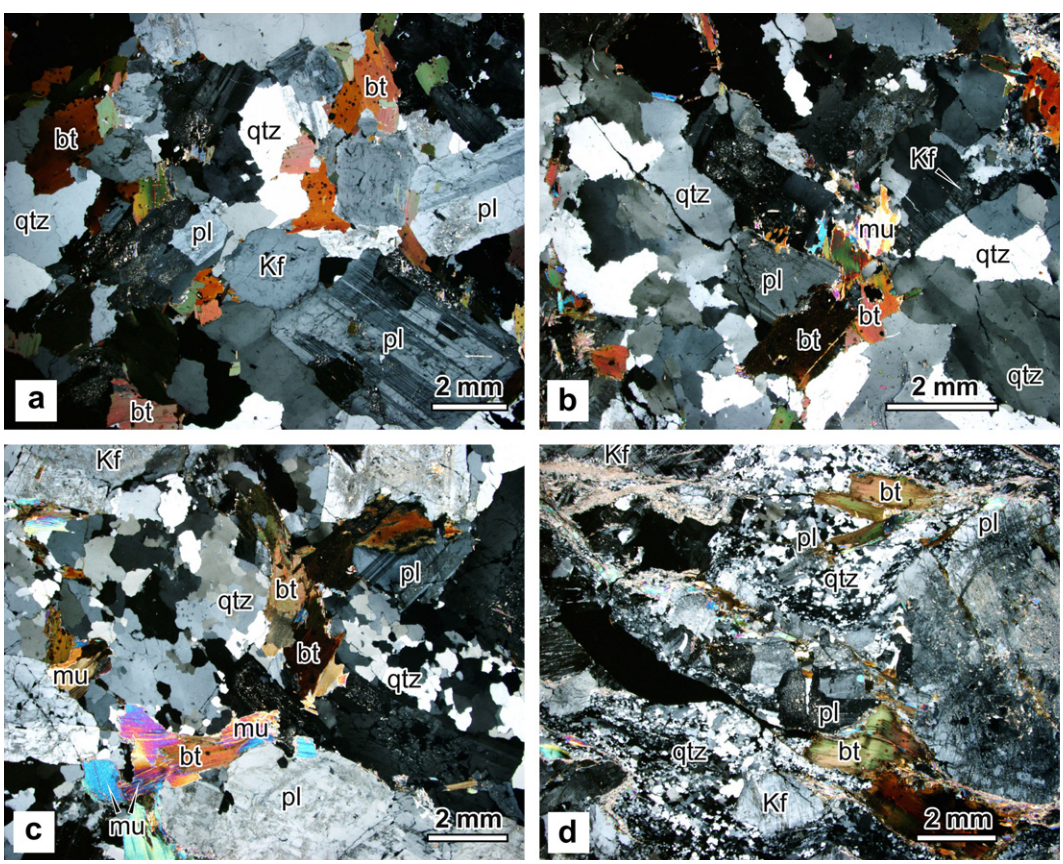

Fig. 5. Four main types of microstructures in the granitoids from the Serra da Estrela – Castro Daire region. Microphotographs under crossed polars. a – Magmatic texture: undeformed biotite and feldspars, no or rare undulatory extinctions and no subgrains in quartz (ES 106); b – Weak submagmatic deformation: sub-boundaries in quartz, rare subgrains of quartz (ES 16); c – Incipient solid-state deformation: frequent sub-boundaries and subgrains in quartz (CD 93); d – Strong solid-state deformation: complete dynamic recrystallization of quartz into small grains, kinked biotites, broken feldspars (CD 61). - bt: Biotite; mu: Muscovite; Kf: K-feldspar; pl.: Plagioclase; qtz: Quartz.

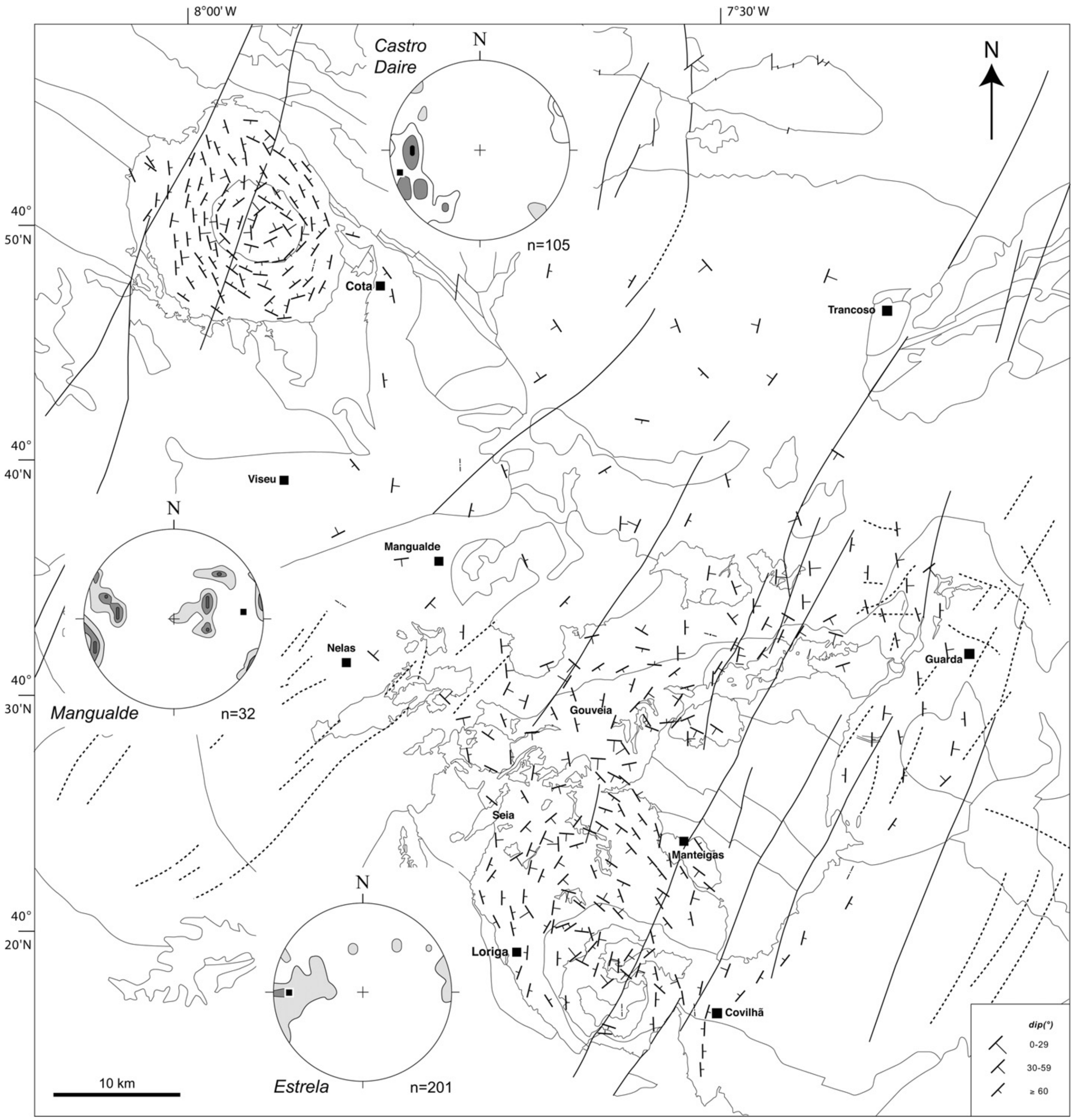

Fig. 6. Map of the magnetic foliations with orientation stereonets for the magnetic foliation poles (Schmidt, lower hemisphere projection, 1% area contours; black square: mean foliation pole).

indicative of moderate solid-state deformation as indicated by the recrystallization of some quartz grains.

4.3. Magnetic fabric patterns

The magnetic fabric, foliation and lineation, is generally parallel to the mineral fabric in the paramagnetic granites (Heller, 1973; Tarling and Hrouda, 1993; Bouchez, 1997). In the studied granites, which display magmatic to submagmatic microstructures, the magnetic foliation and lineation are markers of the flattening and stretching, respectively, of the magmas in the latest stages of their emplacement.

4.3.1. Serra da Estrela granites

The magnetic foliations of the Gouveia, Seia, Loriga and Covilhã quadrangle are concentrically distributed with inward medium to steep dips. The centre of this structure, which we named the Estrela pluton, is located near the highest reliefs of the Serra da Estrela (Fig. 6). To the east of the Estrela pluton, between Covilhã and Guarda, foliations are dominantly NE-SW- to NNE-SSW-striking with rather steep dips, either to the NW or SE. The mean foliation orientation for the Serra da Estrela region is N0°E72°.

The magnetic lineations plunge to the NNW or SSE mainly in the Estrela pluton, but more plunges are to the SSE at medium inclination. To the east of a line connecting the localities of Gouveia and Covilhã, the magnetic lineations are dominantly NE-SW- to N–S-plunging with generally shallow northeast or north plunges (Fig. 7). The regional mean orientation is 170°/33°.

4.3.2. Castro Daire pluton

The magnetic foliations of the peripheral rock facies are concentrically distributed with inward steep dips exceeding 60° typically, except in the NE part where the foliations are very steep and eastward dipping. In the central facies, the foliations are also concentrically distributed but with outward moderate dips displaying a dome-like structure (Fig. 6). The mean orientation for the foliations of this pluton is N164°E80°.

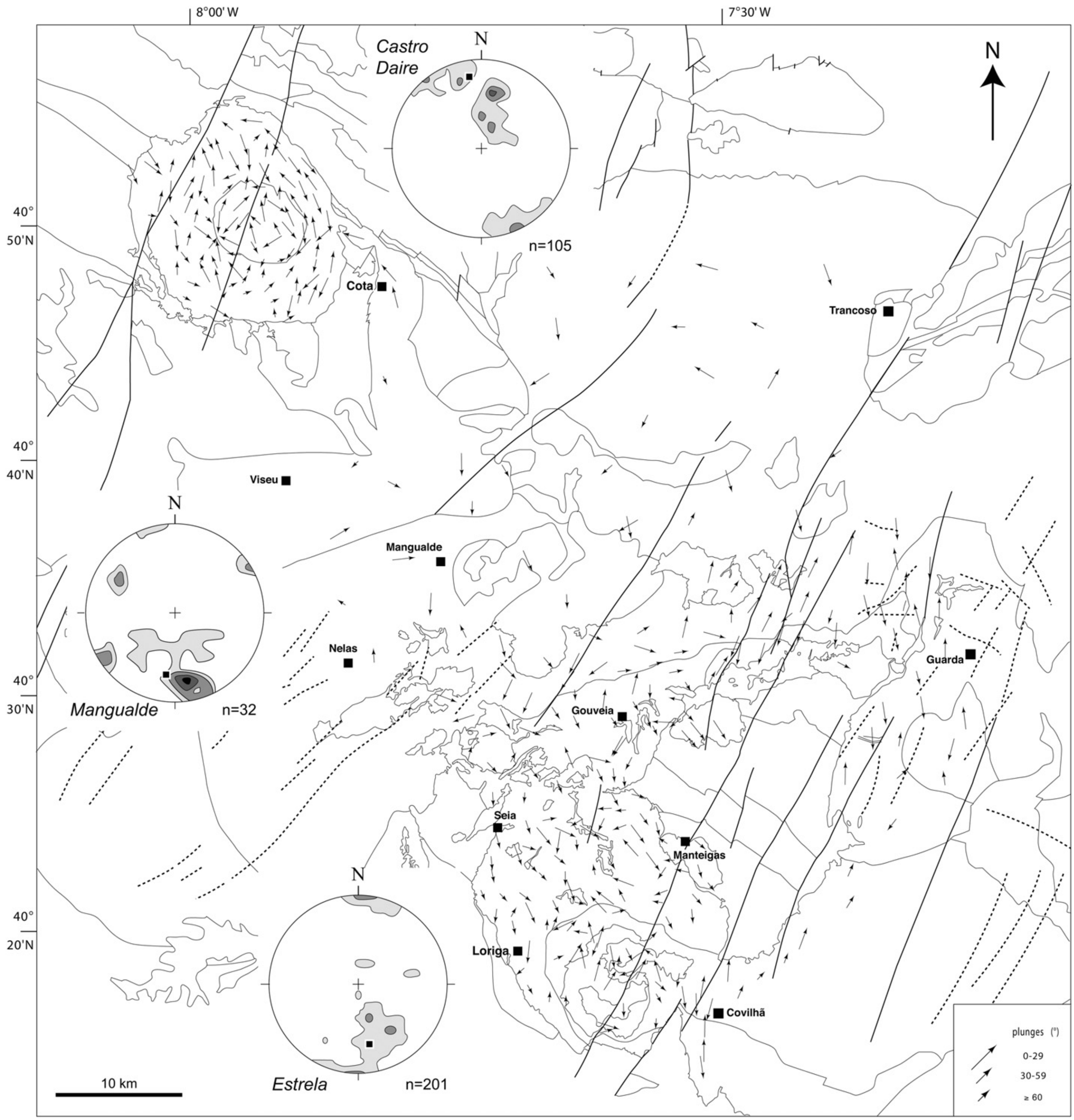

Fig. 7. Map of the magnetic lineations with orientation stereonets for the magnetic lineation (Schmidt, lower hemisphere projection, 1% area contours; black square: mean lineation).

Most magnetic lineations are NNW-SSE-trending with shallow plunges, especially in the central and eastern part of the pluton. To the south, the magnetic lineations are generally NE-SW-trending with shallow to steep plunges (Fig. 7). The mean lineation orientation is 351°/20°.

4.3.3. Mangualde sector

The magnetic foliations are scattered in orientation with a tendency to display an NS-strike with a range of dips (Fig. 6). The mean orientation for the magnetic foliation in this area is N175°W66°.

The magnetic lineations are dominantly NS-trending with shallow to medium plunges. Couto et al. (2003) have measured magnetic foliations and lineations in the Viseu region with an NNW-SSE direction being dominant (Fig. 7). The mean lineation orientation for our sites is 188°/31°.

5. Discussion and interpretation

5.1. Interpretation of the structures of the granitoids of the Serra da Estrela – Castro Daire area

The combination of the different magnetic parameters measured in the granite rocks (*K*m, Ppara%, magnetic fabrics) shows that the area is composed of a complex set of granitoid intrusions. The study of the magnetic susceptibility *K*m allows a characterization of the various granitic types more accurately than with the previous determinations mainly obtained by field observations (Schermerhorn, 1980; de Carvalho et al., 1992; Ferreira and Vieira, 1999). In particular, the Seia and Covilhã granitic facies have the same values of magnetic susceptibility, although they have been represented on the previously published geological maps as different plutons (ref. cit.). Moreover, we found that the Castro Daire and the Estrela plutons have petrographic zonations, rather complex for the Castro Daire pluton, simpler and normal for the Estrela pluton, i.e. from silicic in the center to more mafic on the perimeter.

All the studied granites display in most sites microstructures formed under magmatic or submagmatic state. High to medium temperature solid-state microstructures are not common, indicating that the magnetic fabrics determined by our AMS study correspond to mineral fabrics developed during, or just after, the complete crystallization of the magmas in their sites of emplacement. Syn-emplacement deformation is heterogeneously distributed throughout the area. Zones of rather strong anisotropies (Ppara% $>$ 3.0) occur on the borders of the Estrela pluton, in the Guarda region, in the Mangualde-Cota NS-striking band and in many sites within the Castro Daire pluton. However, zones of strong deformation, such as shear zones, were very scarcely found at the outcrop scale within the granites or in the metasedimentary country rocks.

For the magnetic/magmatic foliations, we found that the two more or less circular intrusive plutons (Estrela and Castro Daire) display steep concentric foliations, and the large granitic zones, without clear boundaries and with medium to steep foliations appear to the east of the Covilhã–Gouveia line, including the Mizarela granite.

The lineations display rather constant orientations over large areas, essentially NNW-SSE and NNE-SSW to N–S, with shallow to moderate plunges. These lineations may be interpreted as stretching directions of the granitic magmas developed during late emplacement (Bouchez, 1997), and are oblique to the NW-SE-striking Douro-Beira sinistral shear zone (Ribeiro et al., 1990; Valle Aguado et al., 2005) and to the ENE-WSW-striking Juzbado-Penalva do Castelo sinistral shear zone (Iglesias and Ribeiro, 1981; Ferreira Pinto et al., 1993) previously identified in this part of the CIZ. The NNW-SSE lineations cover a large region, which includes the eastern part of the Castro Daire pluton, where they are associated with sub-vertical foliations, the Cota-Mangualde zone, and the Estrela pluton. The NNE-SSW lineations occur in the more differentiated facies located in the core of the Estrela pluton, in the granites to the east of the Covilhã–Gouveia line, where they occur with sub-vertical foliations, and to the south and east of the Castro Daire pluton.

Determining the relative ages of the two lineations where they are locally associated, such as in the western part of the peripheral facies of the Castro Daire pluton, is difficult. The NNW-SSE-trending lineations may be interpreted as earlier because they are found in granitic facies that are locally cut by other granitic facies displaying NNE-SSW-trending lineations in the southern part of the Estrela pluton. In their structural study of the region located to the east of Viseu, Couto et al. (2003) also concluded that the "Viseu-Cota" (=Seia) granite which displays NNW-SSE-trending lineations was emplaced before the "Alcafache" (=Covilhã) granite which displays NE-SW lineations. However, the granites displaying different directions of lineations have no clear-cut contacts, pointing out that they were subcontemporaneously co-deformed. In the same way, Azevedo and Nolan (1998), in their study of the Fornos de Algodres granitic intrusions (some km to the NW of Guarda), have considered that this 'granite sequence could have been emplaced within a relatively short range of time with partial overlap between consecutive intrusive phases'.

5.2. Tectonic constraints on the emplacement of the Serra da Estrela – Castro Daire granites

The studied granites are mostly late to post-D3 with an age that is poorly constrained to 308–287 Ma, excluding the special case of the Manteigas granite which could be Ordovician in age (Neiva et al., 2009). The emplacement of these granites, called 'post-kinematic granitoids' by Marques et al. (2002), does not, in fact, postdate the regional tectonics because their syn-emplacement stretching lineations, regularly oriented over large areas and NNW-SSE- to NNE-SSW-trending, should record the evolution of regional

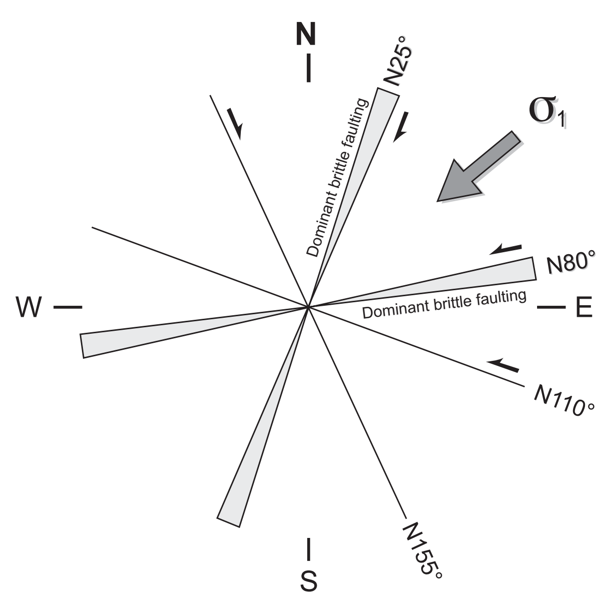

Fig. 8. Geometry and kinematics of the syn-D3 main fault systems according to Marques et al. (2002).

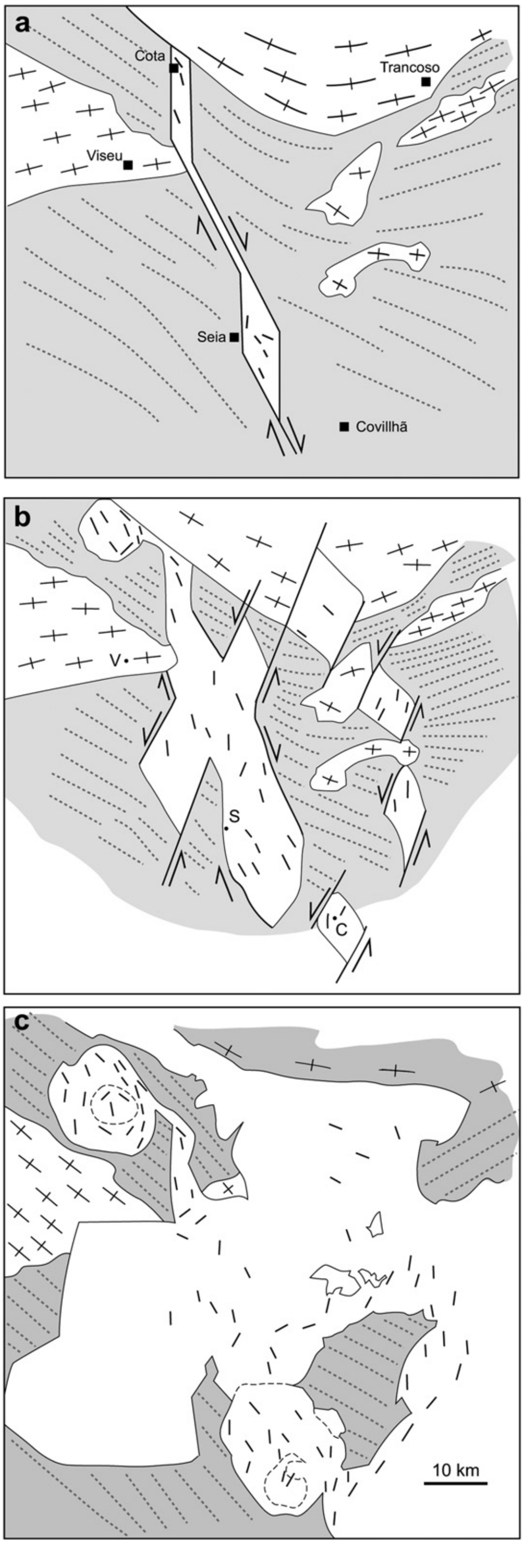

Fig. 9. Kinematic emplacement model of the Serra da Estrela – Castro Daire granites. a – Early granite emplacements. b – Enlargement of the previous zones of granite emplacement, beginning of emplacement of the Castro Daire and Estrela circular plutons and emplacement of granites in the Guarda area. c – Inflation of the granitic plutons mainly due to magma pressure, more or less independently of the tectonics.

strain in the central domain of the CIZ during late-Variscan times. Even so, the tectonic control was only moderate because no related stretching lineations appear in the country rocks. Yenes et al. (1999) reached the same conclusion in their structural study of the La Alberca-Béjar granitic area, located in the Spanish part of the CIZ about 100 km to the east of the Serra da Estrela region.

The two major directions of syn-emplacement stretching lineations, N150 and N20, are generally characterized by shallow plunges in steep foliations, as for example in the northeastern part of the Castro Daire pluton. Such relationships between stretching lineations and foliations point to an emplacement of the granitic magmas dominated by shear strain, possibly related to strike-slip zones roughly parallel to these stretching lineations (see Bouchez, 1997, 2000, for similar examples). However, the corresponding shear senses were not determined because of the weak shape anisotropy of these rocks. Structural data concerning the granites emplaced before and after the late-D3 granites may yield constraints for this problem.

For the syn-D3 granites, possibly emplaced in the 314–307 Ma time-span (see General framework), it has been proposed that their emplacement was related to two main directions of strike-slip faulting, the sinistral N70–80-trending direction (Valle Aguado et al., 2000; Marques et al., 2002) and the dextral N25-trending direction (Ribeiro, 1974; Marques et al., 2002). For the latter, the older dextral N155- and sinistral N110-trending directions of strike-slip faults are considered to play a minor role during this event (Fig. 8).

During the emplacement of the late-D3 granitic rocks the sinistral N70–80-trending direction was almost inactive because no lineations of this direction were found in the intrusions studied here. The N110–120-trending branch was also almost inactive at that time as demonstrated especially by the fact that the Castro Daire pluton does not display fabrics of such orientation, except some solid-state shear bands on its northwestern part, though this pluton was emplaced in country rocks strongly deformed by a sinistral N120 shearing which is therefore older than the pluton emplacement.

Taking into account these data, we propose that the late-D3 granites were emplaced during the reactivation of the N150–155 and N20–25 strike-slip faults inherited from D3. The first direction would be still dextral, whereas the second would be either dextral if during D3, or sinistral if during the emplacement of post-D3 granites (e.g. Vila Pouca de Aguiar pluton, Sant'Ovaia et al., 2000). Likewise, the many NE-SW-striking veins of quartz crosscutting the granites would be release structures corresponding to the N150–155 direction of stretching recorded in these late-D3 granitic rocks.

5.3. Possible mechanism of emplacement of the Serra da Estrela – Castro Daire granites

Granite emplacement is a highly debated question (see de Saint Blanquat et al., 2010, for a recent review) especially concerning the mechanisms (progressive *vs* discontinuous, forceful *vs* passive) and the duration (thousands or millions years) of pluton or batholith construction. The orientation and distribution of the magmatic fabrics that characterize granitic bodies are essential for constraining emplacement interpretations. When no precise dates are available for the various units of a pluton or a batholith, duration of emplacement may be inferred from the nature of the contacts between these units.

Plutons which are interpreted as diapirically emplaced display a circular shape in map view, concentric steep foliations and steep lineations, and show an emplacement-related deformation of their country rock, such as a rim syncline (e.g. He et al., 2009). Such a model of diapiric emplacement does not explain the structures that are observed in this study. Even the circular Castro Daire and Estrela plutons lack evidence of deformation of the country rock related to emplacement or a vertical lineation.

Plutons interpreted as laccoliths are supposed to 'undergo a birth stage, characterized by lateral spreading, followed by an inflation stage marked by vertical thickening' (Petford et al., 2000). In such intrusions, the magmatic foliations are roughly parallel to the contacts with the country rocks, a feature not observed in our study area.

When pluton emplacement is considered to be controlled by tectonics, especially by shear zones, they generally display elongated or rhomb shapes in map view. Their magmatic fabrics, mostly with horizontal lineations and steep foliations, pass progressively to solid-state fabrics toward the borders (Guineberteau et al., 1987; de Saint Blanquat et al., 1998). Only a part of these features, namely the magmatic horizontal or shallow plunging lineations and steep foliations developed at the kilometer scale, are observed in the present region. Therefore, a purely tectonically controlled emplacement of the Castro Daire – Serra da Estrela magmas is not appropriate for explaining all our observations and measurements. Consequently, we believe that the magma pressure also played an important role especially during the last stages of emplacement.

5.4. Model of emplacement of the granites in the Serra da Estrela – Castro Daire area

From the previous data and discussion, we propose a three-stage model of emplacement for the late-D3 granitoids of the Serra da Estrela – Castro Daire region.

- The first stage of emplacement (Fig. 9a) may have been triggered by offsets along the N150-striking dextral strike-slip faults. These movements could have led to local openings in the upper crust favouring the ascent of magmas and the beginning of emplacement of granites, especially along the Cota – Seia zone.
- The second stage (Fig. 9b) may have corresponded to the enlargement of the previously emplaced granites, to the beginning of emplacement of the Castro Daire and Estrela circular plutons and also to the emplacement of granites in the Guarda area related to offsets along possibly sinistral N20-trending strike-slip faults. In this way, these faults could be interpreted as conjugates of the N150-trending faults.
- The third stage (Fig. 9c) may have been characterized by the inflation of the granitic plutons in various directions, more or less independently of the tectonics, leading to their present distribution. In other words, the end of emplacement would be forceful, i.e. essentially related to the magma pressure itself.

The post-emplacement tectonics was just characterized by very local solid-state deformations of the granites and the injection of quartz veins.

6. Conclusion

The present study allows a first structural characterization of a wide outcrop of the late-D3 (or late to post-D3) Variscan granitoids of Central Portugal. The regular fabric patterns here determined demonstrate that granitoid emplacement was controlled by the reactivation of previous crustal-scale strike-slip faults and involved magmatic pressure as a driver. Our structural study points to a rather quick emplacement, whereas the geochronological data indicate that this event might have been c. 20 Ma long (308–287 Ma time-span). More age data could probably help to solve this apparent contradiction. Detailed structural analyses of the late-D3 granites in chosen sites such as the junction of the DBSZ and JPCSZ faults, or the contacts between syn- and late-D3 granites could provide data to improve and refine our model.

Acknowledgements

This study was supported by grants from the French Embassy in Portugal (Project 324 BO) and the Portuguese "Instituto de Cooperação Científica e Tecnológica Internacional" (ICCTI). We thank Ch. Cavaré-Hester for the drawings, A.M. Roquet, F. de Parseval and J.-F. Mena for the thin sections. The manuscript has benefited from constructive reviews by W. Dunne, G. Gutiérrez-Alonso and an anonymous reviewer. We thank J.L. Bouchez, M. de Saint Blanquat, A. Mateus and A. Ribeiro for useful discussions.

References

Arthaud, F., Matte, P.H., 1975. Les décrochements tardi hercyniens du Sud-Ouest de l'Europe. Géométrie et essai de reconstitution des conditions de la déformation. Tectonophysics 25 (1/2), 139–171.

Azevedo, M.R., Nolan, J., 1998. Hercynian late post-tectonic granitic rocks from the Forno de Algodres área (Northern Central Portugal). Lithos 44, 1–20.

Azevedo, M.R., Valle Aguado, B., 2006. Origem e instalação de granitóides variscos na Zona Centro-Ibérica. In: Dias, R., Araújo, A., Terrinha, P., Kulberg, J.C. (Eds.), Geologia de Portugal no contexto da Ibéria. Univ. Évora, Évora, pp. 107–121.

Blumenfeld, Ph., Bouchez, J.L., 1988. Shear criteria in granite and migmatite deformed in magmatic and solid states. Journal of Structural Geology 10 (4), 361–372.

Boorder, H., 1965. Petrological Investigations in the Aguiar da Beira Granite Area, Northern Portugal, Rotterdam, 126 pp.

Bouchez, J.L., 1997. Granite is never isotropic: an introduction to AMS studies of granitic rocks. In: Bouchez, J.L., Hutton, D.H.W., Stephens, W.E. (Eds.), Granite: From Segregation of Melt to Emplacement Fabrics. Kluwer Academic Publishers, Dordrecht, pp. 95–112.

Bouchez, J.L., 2000. Anisotropie de susceptibilité magnétique et fabrique des granites. Comptes Rendus Académie des Sciences de Paris 330, 1–14.

Bouchez, J.L., Bernier, S., Rochette, P., Guineberteau, B., 1987. Log des susceptibilités magnétiques et anisotropies de susceptibilité dans le granite de Beauvoir: conséquences pour sa mise en place. Géologie de la France, BRGM 2–3, 223–232.

Bouchez, J.L., Delas, C., Gleizes, G., Nédélec, A., Cuney, M., 1992. Submagmatic microfractures in granites. Geology 20, 35–38.

Carracedo, M., Paquette, J.L., Alonso Olazabal, A., Santos Zalduegui, J.F., García de Maldinabeitia, S., Tiepolo, M., Gil Ibarguchi, J.I., 2009. U–Pb dating of granodiorite and granite units of the Los Pedroches batholith. Implications for geodynamic models of the southern Central Iberian Zone (Iberian Massif). International Journal Earth Sciences 98, 1609–1624.

de Carvalho, D., Oliveira, J.T., Pereira, E., Ramalho, M., Antunes, M.T., Monteiro, J.H., Collaborators, 1992. Carta geológica de Portugal. Serviços Geológicos de Portugal, Lisboa. Escala 1:500,000.

Couto, A., Valle Aguado, B., Pessoa, J.M., Pinheiro, M., Silva, P.F., Miranda, J.M., Azevedo, M.R., Nolan, J., Medina, J., Martins, M.E., 2003. Anisotropia da susceptibilidade magnética en granitóides hercínicos tardios da região de Viseu (ZCI). Ciências da Terra, Lisboa, V, pp. D25–D28.

Dias, R., Ribeiro, A., 1994. The Ibero-Armorican arc: a collision effect against an irregular continent? In: Dias, R. (Ed.), Regimes de deformação no autóctone da Zona Centro-Ibérica: a importância para a compreensão da génese de Arco Ibero-Armoricano. PhD thesis, Faculdade de Ciências da Universidade de Lisboa.

Diez Balda, M.A., Vegas, R., Gonzalez Lodeiro, F., 1990. Central Iberian zone. Structure. In: Dallmeyer, R.D., Martínez Garcia, E. (Eds.), Pre-mesozoic Geology of Iberia. Springer-Verlag, Berlin, Heidelberg, pp. 172–188.

Diez Balda, M.A., Martínez Catalán, J.R., Ayarza Arribas, P., 1995. Syn-collisional extensional collapse parallel to the orogenic trend in a domain of steep tectonics: the Salamanca Detachment Zone (Central Iberian Zone, Spain). Journal of Structural Geology 17 (2), 163–182.

Escuder Viruete, J., 1998. Relationships between structural units in the Tormes gneiss dome (NW Iberian massif, Spain): geometry, structure and kinematics of contractional and extensional Variscan deformation. Geologische Rundschau 87, 165–179.

Farias, P., Gallastegui, G., Gonzalez Lodeiro, F., Marquinez, J., Martin Parra, L.M., Martínez Catalan, J.R., de Pablo Maciá, J.G., Rodriguez Fernandez, L.R., 1987. Aportaciones al conocimiento de la litoestratigrafia y estructura de Galícia Central. In: IX Reunião de Geologia do Oeste Peninsular, Porto, 1985. Mem. Mus. Labor. miner. geol. Fac. Ciênc. Univ. Porto 1, pp. 411–431.

Ferreira, N., Vieira, G., 1999. Guia Geológico e Geomorfológico do Parque Natural da Serra da Estrela/Carta Geológica Simplificada do Parque Natural da Serra da Estrela. IGM, ICN. Escala 1:75,000.

Ferreira, N., Iglésias, M., Noronha, F., Pereira, E., Ribeiro, A., Ribeiro, M.L., 1987. Granitóides da Zona Centro Ibérica e seu enquadramento geodinâmico. In: Bea, F., Carnicero, A., Gonzalo, J., Lopez Plaza, M., Rodriguez Alonso, M. (Eds.), Geología de los Granitoides y Rocas Asociadas del Macizo Hesperico. Editorial Rueda, Madrid. Libro de Homenaje a L.C. García de Figuerola, pp. 37–51.

Ferreira Pinto, A.F., Gama Pereira, L.C., Regêncio Macedo, C.A., 1993. A zona de cisalhamento dúctil do granito de Sátão: idade e enquadramento geotectónico, vol. 115. Memórias e Notícias, Publ. Mus. Lab. Mineral. Geol., Univ. Coimbra, pp. 57–69.
Gleizes, G., Nédélec, A., Bouchez, J.L., Autran, A., Rochette, P., 1993. Magnetic susceptibility of the Mont-Louis Andorra ilmenite-type granite (Pyrenees): a new tool for the petrographic characterization and regional mapping of zoned plutons. Journal of Geophysical Research 98B, 4317–4331.
Guineberteau, B., Bouchez, J.L., Vigneresse, J.L., 1987. The Mortagne granite pluton (France) emplaced by pull-apart along a shear zone: structural and gravimetric arguments and regional implication. Geological Society of America Bulletin 99, 763–770.
He, B., Xu, Y.G., Paterson, S., 2009. Magmatic diapirism of the Fangshan pluton, southwest of Beijing, China. Journal of Structural Geology 31, 6154–6626.
Heller, F., 1973. Magnetic anisotropy of granitic rocks of the Bergell Massif (Switzerland). Earth Planetary and Science Letters 20, 180–188.
Iglesias, M., Ribeiro, A., 1981. La zone de cisaillement ductile de Juzbado (Salamanca) – Penalva do Castelo (Viseu): Un linéament ancien réactivé pendant l'orogénèse hercynienne? Comunicações dos Serviços Geológicos de Portugal 67 (1), 89–93.
Julivert, M., Fontboté, J.M., Ribeiro, A., Conde, L., 1974. Mapa Tectónico de la Península Ibérica y Baleares. Escala 1: 1,000,000. Memoria Explicativa. Instituto Geológico y Minero de España, Madrid, 113 pp.
Marques, F.O., Mateus, A., Tassinari, C., 2002. The Late-Variscan fault network in central-northern Portugal (NW Iberia): a re-evaluation. Tectonophysics 359, 255–270.
Martínez Catalán, J.R., Arenas, R., Abati, J., Sánchez Martínez, S., Díaz García, F., Fernández Suárez, J., González Cuadra, P., Castiñeiras, P., Gómez Barreiro, J., Díez Montes, A., González Clavijo, E., Rubio Pascual, F.J., Andonaegui, P., Jeffries, T.E., Alcock, J.E., Díez Fernández, R., López Carmona, A., 2009. A rootless suture and the loss of the roots of a mountain chain: the Variscan belt of NW Iberia. Comptes Rendus Geoscience 314, 114–126.
Mota Leite, S., Santos, J., Azevedo, M., 2005. Variscan plutonism in the Castro Daire area (Northern Central Portugal) – constraints from U–Pb geochronology. In: The 6th International Symposium on Applied Isotope Geochemistry, Prague, Czech Republic. Abst. with Prog.
Neiva, A.M.R., Williams, I.S., Ramos, J.M.F., Gomes, M.E.P., Silva, M.M.V.G., Antunes, I.M.H.R., 2009. Geochemical and isotopic constraints on the petrogenesis of Early Ordovician granodiorite and Variscan two-mica granites from the Gouveia area, central Portugal. Lithos 111, 186–202.
Nicolas, A., 1992. Kinematics in magmatic rocks with special reference to gabbros. Journal of Petrology 33 (4), 891–915.
Noronha, F., Ramos, J.M.F., Rebelo, J.A., Ribeiro, A., Ribeiro, M.L., 1979. Essai de corrélation des phases de déformation hercynienne dans le Nord-Ouest Péninsulaire. Bol. Soc. Geol. Portugal 21 (2/3), 227–237.
Paterson, S.R., Vernon, R.H., Tobisch, O.T., 1989. A review criteria for the identification of magmatic and tectonic foliations in granitoids. Journal of Structural Geology 11, 349–363.
Paterson, S.R., Fowler Jr., T.K., Schmidt, K.L., Yoshinobu, A.S., Yuan, E.S., Miller, R.B., 1998. Interpreting magmatic fabric patterns in plutons. Lithos 44, 53–82.
Pereira, E., Ribeiro, A., Meireles, C., 1993. Cisalhamentos hercínicos e controlo das mineralizações de Sn-W, Au e U na Zona Centro-Ibérica, em Portugal. Cuaderno Lab. Xeolóxico de Laxe 18, 89–119.
Petford, N., Cruden, A.R., McCaffrey, K.J.W., Vigneresse, J.L., 2000. Granite magma formation, transport and emplacement in the Earth's crust. Nature 408, 669–673.
Ribeiro, A., 1974 Contribution à l'étude de Trás-os-Montes Oriental. Serviços Geológicos de Portugal. PhD thesis, Memórias dos Serviços Geológicos Portugal 24, 168 pp.
Ribeiro, A., Iglésias, M., Ribeiro, M.L., Pereira, E., 1983. Modèle géodynamique des Hercynides Ibériques. Comunicações dos Serviços Geológicos de Portugal 69 (2), 291–293.
Ribeiro, A., Pereira, E., Dias, R., 1990. Structure in the northwest of the Iberian Peninsula. In: Dallmeyer, R.D., Martínez Garcia, E. (Eds.), Pre-mesozoic Geology of Iberia. Springer-Verlag, Berlin, Heidelberg, pp. 220–236.
Rochette, P., 1987. Magnetic susceptibility of the rock matrix related to magnetic fabric studies. Journal of Structural Geology 9 (8), 1015–1020.
de Saint Blanquat, M., Tikoff, B., Teyssier, C., Vigneresse, J.L., 1998. Transpressional kinematics and magmatic arcs. In: Holdsworth, R.E., Strachan, R.A., Dewey, J.F. (Eds.), Continental Transpressional and Transtensional Tectonics. Geological Society, London, Special Publications, vol. 135, pp. 327–340.
de Saint Blanquat, M., Horsman, E., Habert, G., Morgan, S., Vanderhaeghe, O., Law, R., Tikoff, B., 2010. Multiscale magmatic cyclicity, duration of pluton construction, and the paradoxical relationship between tectonism and plutonism in continental arcs. Tectonophysics. doi:10.1016/j.tecto.2009.12.009.
Sant'Ovaia, H., Bouchez, J.L., Noronha, F., Leblanc, D., Vigneresse, J.L., 2000. Composite-laccolith emplacement of the post-tectonic Vila Pouca de Aguiar granite pluton (northern Portugal): a combined AMS and gravity study. Transactions of the Royal Society of Edinburgh: Earth Sciences 91, 123–137.
Schermerhorn, L., 1980. Carta Geológica de Portugal. Escala 1:50,000. Notícia explicativa da folha 14-C – Castro Daire. Serviços Geológicos de Portugal, Lisboa, 39 pp.
Sousa, M.B., 1971. Litoestratigrafia e estrutura do "Complexo Xisto-Grauváquico ante-Ordovícico" – grupo do Douro (NE de Portugal). PhD thesis, Universidade de Coimbra, Coimbra, 222 pp.
Tarling, D.H., Hrouda, F., 1993. The Magnetic Anisotropy of Rocks. Chapman and Hall, London, 217 pp.
Teixeira, C., 1954. Os conglomerados do Complexo Xisto-Grauváquico ante-silúrico. Comunicações da Sociedade Geológica de Portugal 35, 33–49.
Valle Aguado, B., Martínez Catalán, J.R., Azevedo, M.R., 2000. Structure of the western termination of the Juzbado-Penalva do Castelo shear zone (Western Iberian Massif). Galicia 2000. In: 15th International Conference on Basement Tectonics. Basement Tectonics (Program and Abstracts), vol. 15, pp. 287–291.
Valle Aguado, B., Azevedo, M.R., Schaltegger, U., Martínez Catalán, J.R., Nolan, J., 2005. U–Pb zircon and monazite geochronology of Variscan magmatism related to syn-convergence extension in Central Northern Portugal. Lithos 82, 169–184.
Vigneresse, J.L., Barbey, P., Cuney, M., 1996. Rheological transitions during partial melting and crystallization with application to felsic magma segregation and transfer. Journal of Petrology 37 (6), 1579–1600.
Yenes, M., Álvarez, F., Gutiérrez-Alonso, G., 1999. Granite emplacement in orogenic compressional conditions: the La Alberca-Béjar granitic area (Spanish central system, Variscan Iberian belt). Journal of Structural Geology 21, 1419–1440.
Zeck, H.P., Wingate, M.T.D., Pooley, G., 2007. Ion microprobe U–Pb zircon geochronology of late tectonic granitic-gabbroic rock complex within the Hercynian Iberian belt. Geological Magazine 144 (1), 157–177.